Harbour, S. N., Ditoro, D. F., Witte, S. J., Zindl, C. L., Gao, M., Schoeb, T. R., Jones, G. W., Jones, S. A., Hatton, R. D., & Weaver, C. T. (2020). TH17 cells require ongoing classic IL-6 receptor signaling to retain transcriptional and functional identity. *Science Immunology*, *5*(49), eaaw2262. https://doi.org/10.1126/sciimmunol.aaw2262

Th17 Cells Require Ongoing Classic IL-6 Receptor Signaling to Retain Transcriptional and Functional Identity

Authors:

Stacey N. Harbour[1], Daniel F. DiToro[1], Steven J. Witte[1], Carlene L. Zindl[1], Min Gao[2,3], Trenton R. Schoeb[2], Gareth W. Jones[4,5], Simon A. Jones[4,5], Robin D. Hatton[1], and Casey T. Weaver[1*]

Affiliations:

Departments of [1]Pathology and [2]Genetics, University of Alabama at Birmingham, Birmingham AL 35294, USA

[3]Informatics Institute, University of Alabama at Birmingham, Birmingham AL 35294, USA

[4]Systems Immunity University Research Institute, Cardiff University

[5]Division of Infection and Immunity, School of Medicine, Cardiff University, Cardiff CF14 4XN, Wales, U.K.

* Correspondence: cweaver@uabmc.edu (C.T.W.)

One Sentence Summary:

We report here that, in addition to its role in the induction of Th17 cell development, ongoing classic IL-6 receptor signaling is indispensable for maintenance of the Th17 program, identifying a major mechanism by which Th17 cells are retained despite their tendency to transdifferentiate into Th1-like cells that drive immune-mediated disease.

Abstract:

Acting in concert with TGF-β, IL-6 signaling induces Th17 cell development by programming Th17-related genes via STAT3. A role for IL-6 signaling beyond the inductive phase of Th17 cell development has not been defined, as IL-23 signaling downstream of Th17 cell induction also activates STAT3 and is thought responsible for Th17 cell maintenance. Here, we find that IL-6 signaling is required for both induction and maintenance of Th17 cells; IL-6Rα–deficient Th17 cells rapidly lost their Th17 phenotype and did not cause disease in two models of colitis. Co-transfer of WT Th17 cells with IL-6Rα–deficient Th17 cells induced colitis but was unable to rescue phenotype loss of the latter. High IL-6 in the colon promoted classic, or cis, rather than trans receptor signaling that was required for maintenance of Th17 cells. Thus, ongoing classic IL-6 signaling underpins the Th17 program and is required for Th17 cell maintenance and function.

Main Text:

Introduction

Distinct subsets of effector CD4+ T cells differentiate from multipotent naïve precursors under control of antigen- and cytokine-induced signals. Th17 cells arise from antigen-activated naïve CD4+ T cells in response to TGF-β and IL-6 (*1-4*), the latter inducing a signaling cascade that recruits Janus kinases JAK1, JAK2 and TYK2. These in turn induce tyrosine phosphorylation of both STAT3 and STAT1 (*5*). STAT3 induces the expression of Th17-related genes including *Il17a*, *Il17f*, *Il22*, *Il23r* and the master transcription factor *Rorc* (*6-8*), which itself is a positive regulator of key Th17 genes and a negative regulator of alternative lineage fates (*9-12*). Expression of *Il23r* as well as other Th17-specific genes is required for several Th17-mediated diseases, including inflammatory bowel disease (IBD) (*13-15*), psoriasis (*16*) and ankylosing spondylitis (*17*), and exposure of Th17 cells to IL-23 is critical for Th17 maintenance and pathogenesis (*15*, *18-22*).

Th17 cells are highly plastic (*19*, *23*). Under the influence of IL-12 most Th17 cells rapidly extinguish RORγt expression up-regulate T-bet and a Th1-like program (*19*, *24*, *25*). Although IL-23 has been shown to important for Th17 cell maintenance due to its activation of STAT3, reiterative IL-23 signaling also induces Th17 cells to extinguish *Il17a* and *Rorc* in favor of Th1-related genes (*19*, *24*, *25*). This transdifferentiation of Th17 cells is dependent on both STAT4 and T-bet (*19*, *23*, *26*, *27*). Thus, the balance of cytokines in the local environment play a critical role in Th17 maintenance and function. Although the role of IL-6 in Th17 cell induction is well characterized (*2*, *4*), it is unknown whether ongoing IL-6 signaling contributes to Th17 maintenance, or whether there are additional factors that antagonize lineage-destabilizing signals such as IL-12– and IL-23–induced STAT4 to preserve the Th17 phenotype.

IL-6 is produced by a wide range of cells, including hematopoietic-derived monocytes, macrophages and dendritic cells, and non-hematopoietic stromal cells such as fibroblasts and endothelial cells(*28*). Various inflammatory cytokines (e.g., IL-1 and TNFα) and innate sensing

mechanisms contribute to the generation of IL-6, which elicits a broad range of biological functions on target cells (*29*). Effects range from control of organ development, the regulation of the acute-phase response and immune-related functions such as cell survival, differentiation, proliferation and apoptosis (*30*). The pleiotropic effects of IL-6 are transmitted through a tightly controlled, variable mode of signaling (*31*). Classic, or cis, IL-6 receptor signaling occurs in cells that express both membrane-bound IL-6Rα and the signal transducing component, gp130, which bind IL-6 in a hexameric complex where IL-6, IL-6Rα and gp130 exist in a 2:2:2 stoichiometry (*32*). While gp130 is ubiquitously expressed (*33*), IL-6Rα expression is restricted to hepatocytes (*34*) and subsets of leukocytes, including naïve T cells (*35*). In activated cells that express IL-6Rα, particularly activated neutrophils, monocytes and T cells (*36*), the extracellular domain can be shed by proteolysis to liberate a functional soluble IL-6Rα (sIL-6Rα)(*37*, *38*). Soluble IL-6Rα binds IL-6 to form an agonistic dimer that can bind gp130 to induce IL-6 signaling through a mechanism termed IL-6 trans-signaling. A soluble isoform of gp130 (sgp130) buffers the activity of IL-6 trans-signaling and restricts the bioavailability of IL-6–sIL-6Rα complexes for signaling through membrane-bound gp130 (*39*). Given that gp130 is ubiquitously expressed, the local balance between IL-6, sIL-6Rα and sgp130 IL-6 responsive target cells thus determines the prominent mode of IL-6 signaling acting on any cell type (*40*). A additional form of IL-6 signaling, referred to as trans-presentation, involves binding of the cell suface-asscociated IL-6–sIL-6Rα complexes on a subset of dendritic cells to gp130 expressed on naive T cells, and has been proposed as a mechanism that promotes the development of pathogenic Th17 cells (*41*).

An excess of IL-6 relative to sIL-6Rα in acute injury leads to classic signaling, which is believed to have more homeostatic effects such as the acute phase response (*42*). An excess of sIL-6Rα, however, is a marker of active inflammation (*43*) and allows for trans-signaling to a wide variety of cell targets, and amplifies inflammatory responses through the recruitment and activation of mononuclear cells (*44*, *45*). IL-6 trans-signaling has been shown to affect the recruitment of Th17 cells in model of peritoneal inflammation (*46*), although it is unknown whether these effects were direct or indirect.

Here, we have used a mouse model of Th17 cell-induced colitis (*19*) to examine a possible contribution of IL-6 to Th17 biology beyond the early phase of Th17 induction. We find that expression of IL-6Rα by mature Th17 cells is indispensable for maintenance of the Th17 phenotype and a pathogenic response. Classic IL-6 receptor signaling was dominant over IL-6 trans-signaling in the colon due to the high levels of IL-6 produced there. Our findings establish that ongoing IL-6 is required for maintenance of Th17 cells and suggest that a major contributor to Th17 plasticity is the loss of IL-6 signaling.

Results

Naïve CD4$^+$ T cells require IL-6 signaling for development of colitis

The Th17 pathway is critical to IBD pathogenesis. In view of the requirement for IL-6 in Th17 cell development, we examined whether naïve CD4$^+$ T cells deficient in IL-6Rα were able to develop into Th17 cells and drive intestinal inflammation *in vivo*. WT and *Il6ra*$^{-/-}$ naïve T cells were used as donors in the CD4$^+$ CD45RB^{Hi} T cell transfer colitis model (*47*). Eight weeks after transfer into *Rag1*$^{-/-}$ recipients, T cells from WT mice were found to induce substantial disease. This was reflected by a significant loss of weight (**Fig. 1A**), as well as an increase in CD4$^+$ cells recovered from the colonic lamina propria (CLP) of colitic mice (**Fig. 1B**). While the transfer of WT CD4$^+$ cells resulted in pronounced pathology (**Fig. 1C** and **D**), the transfer of *Il6ra*$^{-/-}$ CD4$^+$ cells failed to induce weight loss or significant colonic inflammation.

Consistent with previous reports, flow cytometric analysis of T cells recovered from the inflamed CLP and mesenteric lymph node (MLN) identified four populations of IL-17A and IFN-γ expressing cells in WT recipients (**Fig. 1G** and **Supplementary Fig. 1**)(*19*). In contrast, there was a significant reduction in the percentage and number of IL-17A$^+$ and IL-17A$^+$IFN-γ$^+$ cells in the CLP (**Fig. 1G,H**) and MLN (**Supplementary Fig. 1**) of recipients of *Il6ra*$^{-/-}$ T cells. Interestingly, the relative percentage of IFN-γ producing cells in *Il6ra*$^{-/-}$ recipient T cells was unchanged in the CLP (**Fig. 1H**) and increased in the MLN (**Supplementary Fig. 1**), but their

numbers were not increased. Thus, IL-6 receptor signaling in these cells is not required for development of an intact Th1 pathway but is essential for control of pathogenic T cells displaying a Th17 program (*15*, *48*). The numbers of $CD4^+$ $Foxp3^+$ cells in the CLP (**Fig. 1E,F**) and MLN (**Supplementary Fig. 1**) remained unchanged between recipients of WT and *Il6ra*$^{-/-}$ cells, suggesting that reduction in disease in *Il6ra*$^{-/-}$ recipients was not due to an increase in Treg cells and suppression of an inflammatory response in the absence of IL-6. Together, these results indicate that IL-6 signaling in naïve $CD4^+$ T cells is required for the pathogenesis of IBD and that trans-signaling in the absence of membrane bound IL-6Rα is not sufficient to induce development of a pathogenic Th17 response. These findings are in agreement with other studies that showed defective Th17 responses in the absence of IL-6Rα (*49*).

Maintenance and pathogenesis of Th17 cells is dependent on ongoing IL-6 signaling

Previous results using IL-6–deficient animals or blocking IL-6 interventions suggest that IL-6 is required to promote Th17-induced disease (*12*, *50*, *51*). However it is currently unknown whether on-going IL-6 signaling is required to maintain Th17 responses. To investigate this, we used a Th17 transfer model of colitis (*19*), wherein Th17 polarized cells are cultured *ex vivo* from naïve $CD4^+$ T cells of *Il17f*$^{thy1.1}$ reporter mice (**Fig. 2A**) and sorted on the basis of Thy1.1 (IL-17F) expression (**Fig. 2B**). Transfer of $Thy1.1^+$ ($IL\text{-}17F^+$) Th17 cells into *Rag1*$^{-/-}$ mice induces a rapid onset of disease that is equivalent in severity to that caused by transfer of $CD4^+$ $CD45RB^{hi}$ T cells (*19*).

Isolated Th17 cells were transferred into groups of *Rag1*$^{-/-}$ or *Il6*$^{-/-}$*.Rag1*$^{-/-}$ mice. When compared to *Il6*$^{-/-}$*.Rag1*$^{-/-}$ recipients, *Rag1*$^{-/-}$ recipients showed significantly elevated disease activity (**Fig. 2C, D**). In this regard, the absence of IL-6 lead to a reduction in the percentage and number of $IL\text{-}17A^+$ $CD4^+$ cells recovered from the CLP of colitic mice (**Fig. 2E, F**). However, the percentage and numbers of double $IL\text{-}17A^+IFN\text{-}\gamma^+$ and single $IFN\text{-}\gamma^+$ cells in *Il6*$^{-/-}$*.Rag1*$^{-/-}$ recipients was comparable to that seen in *Rag1*$^{-/-}$ recipients. The percentage of $CD4^+$ $Foxp3^+$ cells in the CLP of recipient mice was also unchanged (**Supplementary Fig. 2**), suggesting that disease disparity was not due to

elevated Treg numbers in the absence of IL-6. While IL-6 signaling is known to promote anti-apoptotic mechanisms (*44*), Annexin V staining of $CD4^+$ cells recovered from the CLP of colitic *Rag1*$^{-/-}$ and *Il6*$^{-/-}$*.Rag1*$^{-/-}$ recipients showed no difference in the percentage of apoptotic (Annexin V^+ Propidium $Iodide^+$) cells (**Supplementary Fig. 2**), suggesting that the differences observed was not due to a loss of IL-6-mediated T cell survival at this stage of disease. While IL-6 deficient mice are known to have other defects that may inhibit an immune response, particularly in the innate immune compartment, these findings support a role for IL-6 in the maintenance of Th17 responses required for chronic disease progression. We therefore considered the mode of IL-6 receptor signaling responsible for this outcome.

Classic IL-6 signaling is required for maintenance of pathogenic Th17 cells

The previous experiments suggested that ongoing IL-6 signaling is required to maintain a pathogenic Th17 response, but could not discern whether IL-6 was acting via classic versus trans IL-6 signaling to maintain Th17 cells. Because naïve $CD4^+$ T cells from *Il6ra*$^{-/-}$ mice are not responsive to direct IL-6 activation (**Fig. 3A**), we used Th17 cells from *Il6ra*$^{-/-}$ mice as donors in the Th17 transfer colitis model to interrogate the requirement for classic IL-6 receptor signaling. Consistent with our previous work (*46*), under Th17 polarizing conditions, *Il6ra*$^{-/-}$ $CD4^+$ T cells could not produce IL-17A in response to TGF-β+IL-6. However, this lack of IL-6–induced Th17 differentiation was restored by using a recombinant IL-6-sIL–6Ra fusion protein (Hyper-DS-sIL-6R; HDS), which acts exclusively via IL-6 trans-signaling (**Fig. 3B**). Importantly, both IL-6 and HDS generated a similar proportion of Th17 cells when combined with TGF-β (**Fig. 3B, Supplementary Fig. 3**). There was no difference in the proliferative capacity of WT and Il*6ra*$^{-/-}$ Th17 cells *in vitro* as measured by vital dye dilution, and RNA-seq analysis of WT (IL-6), WT (HDS), and *Il6ra*$^{-/-}$ Th17 precursors showed a very high degree of similarity by principal component analysis of gene expression, with only 3 genes being > 1.5 fold differentially expressed with an FDR of < 0.05 (*Serpine2*, *Kit*, *Nav1*) (**Supplementary Fig. 3**). In addition, pSTAT3 levels were equivalent between Th17 cells restimulated with IL-6 or HDS in vitro (**Supplementary Fig. 3**).

Thus, naïve CD4+ T cells display a comparable capacity to differentiate into Th17 cells in response to either classic or trans IL-6 receptor signaling.

Exploiting this dual form of Th17 cell regulation, we next considered the relative importance of these IL-6 receptor signaling mechanisms in maintaining local Th17 responses. Thy1.1$^+$ Th17 precursors from WT (IL-6 polarized), WT (HDS polarized) and *Il6ra*$^{-/-}$ (HDS polarized) CD4$^+$ T-cells were transferred into *Rag1*$^{-/-}$ mice. Disease activity and T cell phenotype were assessed four weeks after transfer. Notably, while Th17 cells from WT mice caused severe disease in *Rag1*$^{-/-}$ recipients, Th17 cells from *Il6ra*$^{-/-}$ mice induced significantly less pathology (**Fig. 3C, Supplementary Fig. 3**). Importantly, there was no difference in the ability of WT (IL-6) versus WT (HDS) Th17 cells to induce disease, suggesting that these cells are functionally comparable. The reduced disease observed in recipients of *Il6ra*$^{-/-}$ Th17 cells was associated with a significant loss of IL-17A$^+$ and IL-17A$^+$IFN-γ^+ T cells recovered from the CLP, with a concomitant increase in the percentage of IFN-γ^+ T cells when compared to recipients of WT Th17 cells (**Fig. 3E,G**). As with disease scores, there were no detectable differences between phenotypes of recovered CD4$^+$ cells from WT (IL-6) and WT (HDS) recipients. Thus, in the absence of IL-6 sustained signaling, Th17 cells were unstable, indicating that ongoing, classic IL-6 signal is required to maintain a Th17 response.

Additionally, there were no differences in the percentage or number of CD4$^+$ Foxp3$^+$ cells in the CLP of *Il6ra*$^{-/-}$ versus WT recipients (**Fig. 3F,H-I**), suggesting that loss of Th17 phenotype is not due to conversion to Treg in the absence of IL-6 signaling. Serum sIL-6Rα, which is elevated during inflammation due to shedding from membrane bound IL-6Rα–expressing cells, was significantly increased in recipients of WT Th17 cells. This was in contrast to recipients of *Il6ra*$^{-/-}$ Th17 cells (**Fig. 3D**), in which serum sIL-6Rα levels were equivalent to untreated *Rag1*$^{-/-}$ mice, suggesting that sIL-6Rα is a marker of disease activity in this model. Importantly, colon explant cultures showed a significant reduction in IL-17A in *Il6ra*$^{-/-}$ Th17 cell recipients, despite showing an increase in IL-23 and IL-21 levels (**Supplementary Fig. 3**), suggesting that these STAT3 inducing cytokines were present but unable to compensate for the loss of IL-6 responsiveness in

$CD4^+$ cells. Together, these results suggest that continued classic IL-6 receptor signaling, rather than IL-6 trans-signaling is required to maintain the pathogenic phenotype of Th17 cells *in vivo*, and that the Th17 phenotype is unstable in the absence of classic signaling.

Loss of Th17 phenotype in *Il6ra*$^{-/-}$ mice cannot be rescued by co-transfer of WT Th17 cells

Coordinate increases of sIL-6Rα and IL-6 potentiate IL-6 trans-signaling. To rule out the possibility that reduced disease in recipients of *Il6ra*$^{-/-}$ Th17 cells (**Fig. 3C**) was due to lack of availability of sIL-6Rα, co-transfer experiments were performed to assess the ability of *Il6ra*$^{-/-}$ Th17 cells to maintain their phenotype in the presence of inflammation induced by WT Th17 cells. Th17 precursors from congenically marked WT and *Il6ra*$^{-/-}$ mice were transferred into *Rag1*$^{-/-}$ recipients either individually or together (WT + *Il6ra*$^{-/-}$ 4 wks), with a fourth group receiving *Il6ra*$^{-/-}$ Th17 cells 2 weeks after WT Th17 cell transfer (WT + *Il6ra*$^{-/-}$ (2 wks)) (**Fig. 4A**).

Four weeks after initial transfer, WT and *Il6ra*$^{-/-}$ Th17 cells in recipients of both (WT + *Il6ra*$^{-/-}$ 4 wks) had repopulated the colon in equivalent numbers (**Supplementary Fig. 4**), suggesting there was no survival advantage by population. Disease severity trended with the total number of recovered CLP $CD4^+$ T cells (**Supplementary Fig. 4**). For example, disease was significantly ameliorated in *Rag1*$^{-/-}$ mice that received single *Il6ra*$^{-/-}$ Th17 cell transfers when compared to recipients of WT Th17 cells (**Fig. 4B, Supplementary Fig. 5**). Both co-transfer groups developed disease that was equivalent to WT recipients, reflecting the increased total number of pathogenic $CD4^+$ T cells in these mice. $CD4^+$ T cells recovered from the CLP of recipient mice showed that regardless of whether they were transferred individually or with WT cells, *Il6ra*$^{-/-}$ Th17 cells failed to retain their Th17 identity, as evidenced by a significant reduction in the percentage of IL-$17A^+$ and IL-$17A^+$IFN-γ^+, as well as IL-$17A^+$TNF-α^+ and IL-$17A^+$GM-CSF^+ $CD4^+$ T cells compared to recipients of WT cells (**Fig. 4C-D** and **Supplementary Fig. 4**). This correlated with a significant reduction in the numbers of IL-$17A^+$ and IL-$17A^+$IFN-γ^+ T cells recovered from the majority of *Il6ra*$^{-/-}$ transfer recipients (**Fig. 4C**).

Importantly, loss of the Th17 phenotype by *Il6ra*$^{-/-}$ cells occurred as early as 2 weeks post transfer (**Fig. 4D**, **bottom panel**, and **Supplementary Fig. 4**). And while the percentage of IFN-γ^{+} cells was increased (and IL-17A^{+} cells lost) in the CLP of *Il6ra*$^{-/-}$ Th17 cell recipients in both co-transfer groups, the number of IFN-γ^{+} cells was significantly decreased compared to WT cells in all groups except that of WT + *Il6ra*$^{-/-}$ cell recipients (4 wks).

The balance between classic IL-6 receptor signaling and IL-6 trans-signaling is tightly controlled by the bioavailability of IL-6, sIL-6Rα and sgp130. These were therefore quantified in serum and colon explant cultures from recipient mice (**Supplementary Fig. 4**). Significant differences were found: Molar ratios of each analyte showed that systemic sIL-6Rα was in excess of both IL-6 and sgp130 in all recipient groups (**Fig. 4E-F**)—a stoichiometry that favors IL-6 trans-signaling. Conversely, colon explant cultures showed that IL-6 was in molar excess relative to sIL-6Rα in all groups (**Fig. 4E**), while sIL-6Rα was again in excess of sgp130 (**Fig. 4F**)—enabling both classic and trans-signaling in the colon microenvironment.

IL-6 signaling promotes T cell proliferation and inhibits apoptosis via its actions to increase Bcl-2(*52*). We therefore measured cell cycling in WT and *Il6ra*$^{-/-}$ Th17 cells following transfer. There were no differences in either BrdU^{+} or Ki67^{+} T cells isolated from the spleens and MLNs (**Supplementary Fig. 5**) of recipient *Rag1*$^{-/-}$ mice 7 days after transfers of WT, *Il6ra*$^{-/-}$ or co-transferred WT + *Il6ra*$^{-/-}$ Th17 cells. From this we inferred that there was no difference in the proliferative capacity of *Il6ra*$^{-/-}$ Th17 cells, whether transferred individually or co-transferred with WT Th17 cells. Similarly, there were equivalent percentages of CD4^{+} T cells from the CLP and MLN (**Supplementary Fig. 5**) that were BrdU^{+} and Ki67^{+} four weeks after transfer, suggestive of no defect in the proliferative capacity of *Il6ra*$^{-/-}$ Th17 cells in active colitis. Interestingly, nearly 70% of CLP T cells from *Il6ra*$^{-/-}$ Th17 recipients were BrdU^{+} four weeks after transfer, even though these cells were not pathogenic. Immunofluorescent staining of colon sections from WT + *Il6ra*$^{-/-}$ recipients showed that WT and *Il6ra*$^{-/-}$ Th17 cells repopulate the colon equivalently at 4 weeks post transfer (**Fig. 4G-H**), indicating no defect in the ability of *Il6ra*$^{-/-}$ Th17 cells to traffic to the colon.

Together, these findings establish that persistent IL-6 signaling is required to maintain the Th17 phenotype *in vivo*, and that classic rather than trans IL-6 receptor signaling is favored for maintenance of the Th17 program in the colon microenvironment; the requirement for IL-6 signaling is not related to effects on cell cycle or cell survival, but instead appears to be intrinsic to Th17 lineage maintenance.

IL-6 trans-signaling activates STAT1 and STAT3 in IL-6Rα-deficient Th17 cells *ex vivo*

IL-6 signaling activates the transcription factors STAT3 and STAT1 in naive CD4$^+$ T cells, and studies have shown that CD4$^+$ T cell activation status can alter the balance of STAT3/STAT1 activation downstream of IL-6 signaling (*53*, *54*). *Il6ra*$^{-/-}$ Th17 cells appeared to be either unresponsive or unable to receive IL-6 trans-signaling *in vivo* **(Fig. 4)**. To determine whether this might be due to a lack of inflammation-driven availability of the IL-6–IL-6Rα complex or unresponsiveness of Th17 cells to this complex, we co-transferred congenically marked Thy1.1$^+$ Th17 cells from WT and *Il6ra*$^{-/-}$ mice into *Rag1*$^{-/-}$ recipients. Four weeks after transfer, we examined the responsiveness of recovered MLN T cells to IL-6 or HDS *ex vivo*.

Overall, responsiveness to IL-6 signaling was lower in *ex vivo* T cells compared to naïve T cells (**Fig. 5A,B**), due at least in part to reduced expression of IL-6Rα and gp130 on recovered cells (**Supplementary Fig. 6**). IL-6 trans-signaling mediated by HDS induced both pY-STAT3 (**Fig. 5A,B**) and pY-STAT1 (**Fig. 5C,D**) in a small but significant fraction of both WT and *Il6ra*$^{-/-}$ T cells stimulated *ex vivo*, although the percentage of cells positive for pY-STAT3 was substantially higher than those positive for pY-STAT1. In contrast, only WT CD4$^+$ T cells were responsive to classic IL-6 signaling *ex vivo*. IL-6 stimulation induced pY-STAT3 in a significant fraction of WT cells, but, interestingly, did not induce pY-STAT1 in the same population, indicating that, unlike naïve precursors, coupling of the IL-6 receptor to STAT1 via classic signaling is lost in Th17 cells.

Collectively, these data show that both WT and *Il6ra*$^{-/-}$ CD4$^+$ T cells are responsive to trans-signaling *ex vivo*, but this is limited by diminished gp130 expression, consistent with activation-

induced downregulation of gp130 in CD4+ T cells (*53*, *55*, *56*). Moreover, classic IL-6 receptor signaling in WT cells, which promotes retention of the Th17 phenotype, preferentially induces pY-STAT3 without pY-STAT1. Therefore, ongoing classic IL-6 signaling in Th17 cells is required to maintain tyrosine phosphorylation of STAT3, and thus IL-6-induced STAT3 activation is critical for both the development and maintenance of Th17 cells.

Maintenance of the Th17 transcriptional program is dependent on ongoing IL-6 receptor signaling

To further characterize the phenotypic divergence of *Il6ra*$^{-/-}$ Th17 cells, we performed RNA-sequencing analysis of T cells that were isolated from the CLP of *Rag1*$^{-/-}$ mice that received co-transfers of congenically marked WT and *Il6ra*$^{-/-}$ Th17 cells (**Fig. 6A**). Recipient mice were repopulated with equivalent percentages (**Fig. 6B**) and numbers (**Fig. 6C**) of Th17 cells in the CLP four weeks after transfer. Transcriptome analysis revealed a number of differences in gene expression in recovered WT and *Il6ra*$^{-/-}$ CD4+ T cells *ex vivo* (**Fig. 6D**). Gene set enrichment analysis (GSEA) using a previously defined Th17–Th1 gene set (*57*) identified significant enrichment of Th1-related genes in *Il6ra*$^{-/-}$ T cells *ex vivo* (**Fig. 6E**, **right** and **Supplementary Fig. 7**). Conversely, and in accord with our previous findings, the transcriptome of WT T cells was enriched for a subset of genes related to Th17 cells *ex vivo* (**Fig. 6E**, **left** and **Supplementary Fig. 7**). Signature Th17 related genes that were retained in WT but not *Il6ra*$^{-/-}$ T cells *ex vivo* included *Il17a*, *Il17f*, *Il21*, *Il22*, *Il23r*, *Rorc* and *Ccr6* (**Fig. 6F**). A number of Th1-related genes was enriched in *Il6ra*$^{-/-}$ T cells, including *Ifng*, *Tbx21* and *Il12rb2*, indicative of a molecular program more similar to Th1 cells than the Th17 precursors. GSEA using a dataset derived from colonic CD4+ T cells (GSE58147)(*58*) showed the expression pattern of WT and *Il6ra*$^{-/-}$ CD4+ T cells was significantly related to that of WT and *Il23r*$^{-/-}$ CD4+ T cells, respectively (**Supplementary Fig. 7**). Likewise, a subset of genes induced by *Tbx21* was significantly associated with *Il6ra*$^{-/-}$ T cells (**Supplementary Fig. 7**), consistent with the transdifferentiation of these cells to a Th1-like program.

Using a previously published dataset defining the transcriptional program of Th17 cells (*9*), significant enrichment of *Stat3*- and *Rorc*-induced genes was found in WT T cells *ex vivo*, as expected, whereas *Stat3*- and *Rorc*-repressed genes were significantly enriched in *Il6ra*$^{-/-}$ T cells (**Fig. 6G-J**). In addition, expression of genes regulated by other transcription factors associated with the Th17 lineage, including *Batf*, *Irf4*, *Fosl2* and *Hif1a*, was significantly reversed in *Il6ra*$^{-/-}$ T cells *ex vivo* (**Supplementary Fig. 7**), in fitting with the loss of Th17 phenotype in these cells. As expected, the *Stat3*- and *Rorc*-induced genes enriched in WT cells contained some overlap, including *Il17a*, *Il17f*, *Il23r*, *Il1r1* and *Lif* (**Fig. 6H**,**J**). Interestingly, there was little overlap in genes repressed by *Stat3* and *Rorc* in *Il6ra*$^{-/-}$ CLP T cells. Targets of *Rorc* included *Ahr*, *Ccr5* and *Il12rb2* **(Fig. 6H)**, while *Stat3* repressed genes included *Fasl*, and the Th1-related transcription factors *Tbx21* and *Irf1* (**Fig. 6J**). This is consistent with data suggesting that *Stat3* is a key transcriptional activator in Th17 cells, whereas *Rorc* is thought to be an expression modulator (*9*).

Our previous work has shown that Th17 cells develop divergent gene expression profiles under the influence of IL-23 signaling (*19*), such that an increase in expression of *Tbx21*, *Ifng*, *Ccr5* and *Fasl* is correlated with a significant portion of IFN-γ–producing ex-Th17 cells, whilst a decrease in the expression of *Il17a*, *Il17f*, *Ccr6* and *Ccl20* is correlated with a reduction in IL-17A^{+} Th17 cells. We find here that *Il6ra*$^{-/-}$ CLP CD4^{+} T cells were enriched for the aforementioned Th1 genes. Conversely, expression of Th17-related genes was associated with WT, rather than *Il6ra*$^{-/-}$ CLP CD4^{+} T cells, further indicating that ongoing IL-6 signaling is required to maintain Th17 program stability. Taken together, these data confirmed our finding that *Il6ra*$^{-/-}$ Th17 cells rapidly lose their Th17 phenotype *in vivo*, and extended them to show that, absent classic ongoing IL-6 signaling, the entire Th17 gene expression program is downregulated, favoring the transition of many cells to a Th1-like program.

Enforced RORγt expression in IL-6R-deficient Th17 cells supports maintenance of the Th17 program but does not completely prevent Th1 transdifferentiation

A critical gene target of IL-6 signaling in Th17 cells is *Rorc*, which underpins the Th17 gene expression program while inhibiting alternative programs. Important functions of IL-6/STAT3-induced RORγt include inhibition of IFN-γ/STAT1 and IL-12/STAT4 via suppression of T-bet (*61*), although RORγt also sustains expression of *Il23r*, which has been shown to be central to the transdifferentiaiton of Th17 cells into Th1-like cells *in vivo* via STAT4 signaling (*19*, *26*, *73*). Our gene expression analysis showed that in IL-6Rα-deficient Th17 cells, *Rorc* and *Il23r* expression were rapidly lost along with other genes of the Th17 program following adoptive transfers (**Fig. 6F**). To determine whether loss of RORγt was responsible for loss of the Th17 phenotype, we polarized congenically marked naïve WT and *Il6ra*$^{-/-}$.*Il17f*$^{Thy1.1}$ T cells under Th17 conditions with HDS and transduced cells with retroviruses that expressed GFP alone or GFP plus RORγt at 24 hrs of a 5 day culture (**Fig. 7A**). As expected, Th17 precursors from both WT and *Il6ra*$^{-/-}$ mice expressed a higher percentage of IL-17A after enforced RORγt expression (**Fig. 7B, right**). GFP^{+}Thy1.1^{+} Th17 cells were sorted 4 days after transduction and WT Th17 cells expressing GFP alone (WT pMIG) were transferred together with either *Il6ra*$^{-/-}$ cells expressing GFP alone (*Il6ra*$^{-/-}$ pMIG) or *Il6ra*$^{-/-}$ cells expressing both GFP and RORγt (*Il6ra*$^{-/-}$ pMIG-RORγt) into *Rag1*$^{-/-}$ recipients.

Three weeks after transfer, both co-transfer groups had developed comparable disease (**Fig. 7C, 7F**). CD4^{+} T cells recovered from the CLP showed that, consistent with previous results (**Fig. 4**), Th17 cells transfected with empty vector (*Il6ra*$^{-/-}$ pMIG) rapidly lost their Th17 phenotype as shown by a significant reduction in IL-17A^{+} cells compared to co-transferred WT (WT pMIG) Th17 cell controls (**Fig. 7D and E**), with a concomitant increase in the relative frequency of IFN-γ^{+} cells. In contrast, *Il6ra*$^{-/-}$ Th17 cells transfected with RORγt (*Il6ra*$^{-/-}$ pMIG-RORγt) had a much greater propensity to retain their Th17 phenotype even in the absence of classical IL-6 signaling. Thus, the frequencies of both IL-17A^{+} and IL-17A^{+} IFN-γ^{+} cells from recipients of RORγt-transfected *Il6ra*$^{-/-}$ Th17 cells were markedly increased in comparison to those transduced with vector alone (**Fig. 7D and E**). Moreover, RORγt-transfected Th17 cells had significantly greater retention of IL-17 expression compared to WT controls, reflecting the role of RORγt in promoting Th17

cytokine production (*12*). Interestingly, although RORγt-transfected *Il6ra*$^{-/-}$ Th17 cells had significantly decreased expression of IFN-γ compared to *Il6ra*$^{-/-}$ Th17 cells transfected with empty vector, they showed a modest, but significant increase in the fraction of IFN-γ^{+} cells compared to WT Th17 cells. This is consistent with the development of Th1-like cells from the larger frequency of Th17 precursors maintained by exogenous RORγt (*19*), but also suggested that enforced RORγt expression did not entirely repress transdifferentiation of Th17 cells into Th1-like cells.

In accord with the phenotypic data, gene expression analysis of CD4^{+} T cells recovered from CLP showed that RORγt-transfected *Il6ra*$^{-/-}$ Th17 cells had a significant increase in expression of genes of the Th17 program compared to empty-vector *Il6ra*$^{-/-}$ Th17 cells, including *Il17a*, *Rorc*, *Il17f* and *Il23r* (**Fig. 7G**). Further, there was decreased *Il12rb* but not *Tbx21*, suggesting differential sensitivities of these two genes to RORγt-mediated repression. Notably, expression of *Rorc* was not significantly increased over that of recovered WT controls, indicating the levels of RORγt driven by retroviral transduction were physiologic. As anticipated, *Il23r* was significantly elevated in RORγt-transfected *Il6ra*$^{-/-}$ Th17 cells compared to both empty-vector *Il6ra*$^{-/-}$ cells and co-transferred WT control cells, consistent with an central role for IL-6–induced RORγt in the maintenance of *Il23r* expression. As IL-23 signaling via STAT4 is known to be a principal pathway mediating the transdifferentiation to Th1-like cells *in vivo* (*19*, *26*), it is likely that the elevated expression of IL-23R by RORγt-transfected *Il6ra*$^{-/-}$ Th17 cells contributed to the modest increase in expression of IFN-γ by these cells compared to WT controls, despite on-going RORγt expression. Together, these results suggest that ongoing classical IL-6 signaling supports the Th17 program by sustaining RORγt expression that contributes to the maintenance of Th17 cells, which provide a reservoir of cells that can transdifferentiate into pathogenic Th1-like cells that are essential to colitogenesis.

Discussion

IL-6 is required for lineage specification of Th17 cells through its activation of STAT3, which antagonizes the IL-2/STAT5-driven specification of induced Treg cells with which Th17 cells share TGF-β–dependent developmental programming (*62-64*). Here, we report that in addition to its key role in Th17 cell induction (*3*, *4*), there is an absolute requirement for persistent IL-6 signaling to maintain the Th17 genetic program, and thus Th17 cells. Although it has been reported that IL-23 signaling is important for the maintenance of Th17 cells (*18*, *19*, *21*), we find that ongoing IL-6 signaling is indispensable and foundational, acting upstream of IL-23 via its unique function to sustain RORγt expression and thereby IL-23R expression. Importantly, although Th17 cells were fully competent to receive IL-6 trans-signaling, classic IL-6 signaling proved necessary for Th17 maintenance in the uninflamed and inflamed intestines. This appears to be due to the combined effects of high local production of IL-6, which was incompletely buffered by soluble IL-6Rα, and the abundance of gp130-expressing non-T cells (e.g.., intestinal epithelial cells), which act as a sink for trans-signaling. Possible differences between the classic and trans-signaling modes may also be contributory and deserve further study.

In contrast to Th1 and Th2 cells, Th17 cells show substantially greater plasticity (*19*, *23*, *65*). This reflects intrinsic instability in the transcriptional circuit upon which Th17 cell development is based. Whereas the Th1 and Th2 programs are reinforced by cell-extrinsic and -intrinsic mechanisms that enhance expression of T-bet and GATA-3, respectively(*66*), mechanisms by which RORγt expression is sustained and the Th17 program maintained have been unclear. IL-23 has been reported to be a trophic factor for Th17 cells (*19*, *23*, *65*), but IL-23 signaling also promotes the transdifferentiation of Th17 cells to Th1-like cells (*19*, *26*), thereby contributing to the instability of Th17 cells. Despite its dominant activation of STAT3, IL-23 signaling also activates STAT4, leading to expression of T-bet, which represses RORγt via direct binding to the *Rorc* locus (*26*, *61*). Our finding that Th17 cells require tonic or intermittent classic IL-6 signaling, which shifts from a STAT3–STAT1 output during early development to a pure STAT3 output in mature cells, indicates that this pathway of STAT3 activation may be essential to counterbalance

the STAT4 output of the IL-23 (or IL-12) receptor to sustain RORγt and the Th17 program. However, it also appears that the IL-6–dependent maintenance of a pool of Th17 cells provides precursors from which pathogenic Th1-like cells can arise. In view of the findings herein, it would appear that stable expression of RORγt does not completely block Th1 reprogramming, consistent with a dominant role of T-bet in overriding the Th17 program.

In view of the role for STAT1 in modulating the STAT3-dominant output of the IL-6 receptor via formation of STAT3-STAT1 heterodimers (*67*), results herein suggest that the maintenance of mature Th17 cells via classic signaling may be strictly dependent on STAT3 homodimers. Moreover, as STAT1 signaling impairs Th17 programming (*59*), the loss of STAT1 activation in Th17 cells receiving classic IL-6 signaling may further reinforce maintenance of the Th17 program. Because trans IL-6 signaling in Th17 cells retained a STAT1 output, which can also induce T-bet expression, it is possible that Th17 cells exposed to this mode of IL-6 signaling may be less resistant to transdifferentiaion mediated by Th1-promoting cytokines that preferentially activate STAT1 (e.g. IFNs) or STAT4 (e.g. IL-12). This will require further study. Notably, despite its elevated expression in the colons of recipients of IL-6Rα-deficient Th17 cells, IL-21, which also activates STAT3 and has been implicated as an autocrine factor for Th17 cells (*8*, *68*), was also unable to compensate for deficiency of IL-6 signaling in maintenance of the Th17 program. The basis for the developmentally-linked shift in STAT activation by the IL-6 receptor and insufficiency of autocrine IL-21 to substitute for IL-6 signaling will also require further study. In any case, collectively, these findings suggest that the local balance of IL-6 and IL-23 is critical in sustaining or destabilizing the Th17 program, resulting a protective versus pathogenic Th17 response.

The finding of a critical requirement for paracrine IL-6 in both the induction and maintenance of Th17 cells draws a further parallel between Th17 cells and Treg cells (*62*). Treg cells require IL-2 for both their development and maintenance (*69*), but are unable to produce IL-2 themselves. Instead, they are thought to rely on production of IL-2 by activated naive or other effector T cells (*69*), akin to the reliance of Th17 cells on IL-6 produced by innate immune cells. For both lineages,

the dependence on a single cytokine as both developmental inducer and maintenance factor renders them particularly susceptible to lineage instability. Moreover, as these two cytokines are cross-inhibitory—IL-6 promotes the development of Th17 cells and inhibits Tregs, while IL-2 promotes the development of Tregs and inhibits Th17 cells—this suggests that competition for their respective inductive/maintenance cytokine is a major contributor to Th17 versus Treg pool size both at homeostasis and during the emergence and subsidence of an antigen-driven inflammatory response. This is of particular importance in intestinal tissues, which are enriched in both Th17 and Treg cells and are subject to ongoing antigenic stimulation from the intestinal microbiome (*70*). In view of the current data that implicate importance of the balance of these cytokines in controlling Th17–Treg cell balance during both an evolving and waning antigenic response, it will be important to better define the precise sources and dynamics of IL-2 and IL-6 production.

The relative contribution of Th17 and Th1 cells to immune-mediated diseases has been an area of considerable interest. Early seminal studies identified a definitive link between Th1 cells and colitis (*47*, *71*), whereas subsequent studies established an essential role for the IL-23–Th17 axis in disease pathogenesis (*15*, *72*). A recent study from our group reconciled these findings by demonstrating that Th1-like cells, which derive from Th17 precursors contingent on intact IL-23-induced STAT4 activation and T-bet expression, were critical for colitis development (*73*). A notable feature of our current findings is that IL-6Rα-deficient Th17 cells more readily transitioned to IFN-γ–producing Th1 cells *in vitro* yet failed to cause colitis *in vivo*. Although this appears to contradict a requirement for Th1 cells in the pathogenesis of IBD, our previous studies showed that Th17 cells assisted the development and/or survival of pathogenic Th1 cells that were unable to drive disease on their own (*73*). While the basis for Th17-mediated support for *de novo* Th1 development remains to be defined, a trivial explanation for the observed lack of disease may be that the rapid loss of Th17 cells unable to receive IL-6 signaling resulted in an inadequate number of Th17 precursors to give rise to sufficient Th1-like cells or promote their *de novo* development.

In light of a critical role for ongoing, classic IL-6 signaling in Th17 maintenance, a more detailed understanding of the dynamics of IL-6Rα and gp130 expression by Th17 cell populations

is needed, as is a better understanding of factors regulating the local concentrations of sIL-6Rα, IL-6 and sgp130 in specific tissue microenvironments such as the intestines. While we and others have found that IL-6Rα and gp130 are downregulated upon T cell activation (*31*), the mechanisms are different. IL-6Rα appears to be downregulated primarily by cleavage of the extracellular domain by the metalloproteinases ADAM10 and ADAM17 in humans (*74*), or only ADAM 10 in mice (*75*), which would appear to favor a shift from classic to trans IL-6 signaling in developing Th17 cells. Surface expression of gp130 is downregulated by internalization, alternative splicing of the encoding mRNA to favor the secreted form, and/or other unidentified mechanisms (*31*). While IL-2 signaling has been shown to inhibit expression of *Il6ra* and *Il6st* (gp130)(*76*), little else is known about conditions that promote retention or re-expression of IL-6Rα and gp130 by T cells, which now appear to be key in determining which cells are competent to retain the Th17 program and by what mode of IL-6R signaling. Although IL-6 trans-signaling was intact and comparable in WT and IL-6Rα-deficient T cells recovered from colitic mice, it was substantially diminished, reflecting diminished gp130 expression and/or signaling competency. This impacted classic signaling in WT cells as well and suggests that mechanisms controlling the expression of gp130 by effector T cells are limiting for Th17 maintenance—irrespective of the expression of IL-6Rα and the local balance of free versus sIL-6Rα-bound IL-6.

Although IL-6 trans-signaling was fully sufficient to differentiate Th17 cells *in vitro*, it was insufficient for either Th17 development or maintenance *in vivo*, despite elevated sIL-6Rα. The reasons for this are unclear, but are unlikely to involve complete buffering by sgp130, as sIL-6Rα was in substantial excess in colitic mice. Rather, competition from intestinal innate, epithelial and stromal cells, all of which can express gp130 and can signal in trans, appeared to prevent IL-6 trans-signaling in Th17 cells. At least in the colon, a high IL-6–sIL-6Rα ratio due to high local production of IL-6 favored sufficiently high concentrations of free IL-6 to enable classic signaling to the relatively small percentage of T cells co-expressing membrane bound IL-6Rα and gp130. Interestingly, the stoichiometry of IL-6–IL-6Rα was comparable in both the homeostatic and inflamed intestines, consistent with a dominant role for classic signaling in Th17 maintenance in

this tissue both at baseline and in the diseased state. Whether this is a common feature of mucosal and non-mucosal barrier tissues is unknown.

An association between polymorphisms in the *IL6RA* gene and susceptibility to both RA and IBD have been found (*77*, *78*). The *IL6RA* variant rs2228145, which leads to increased proteolytic cleavage of IL-6Rα and thus a reduction in membrane-bound IL-6Rα in favor of increased serum levels (*79*) is associated with reduced risk of both RA (*77*) and IBD (*78*). Although the mechanism of protection remains to be characterized, it is possible that it involves both increased buffering of free IL-6 as well as reduced expression of cell surface IL-6Rα, such that classic signaling required for Th17 development, and thus disease induction, is impaired. Given the findings herein, it is possible that this variant also compromises the maintenance of Th17 cells.

Our finding that ongoing IL-6 signaling is required for Th17 maintenance has implications for therapeutics that target Th17-mediated diseases. In systemic Th17-related autoimmune diseases such as rheumatoid arthritis, juvenile idiopathic arthritis, and systemic sclerosis, treatment with biologics that inhibit IL-6 is an effective or promising therapy (*80-82*). This is in contrast to tissue-specific immune-mediated diseases, including IBD, where therapies that inhibit IL-6 signaling have not gained clinical use despite evidence that antibodies targeting IL-6 or IL-6Rα may have efficacy (*83*). Given that IL-17A- and IL-22-producing Th17 cells appear to be protective rather than pathogenic in the intestines (*84*), persistent classic IL-6 receptor signaling that sustains intestinal Th17 responses may enhance barrier function to restrain disease. This is in line with the view that classic and trans-signaling promote anti- and pro-inflammatory responses, respectively (*85*), and suggests that inhibiting classic signaling and thus the protective effects of IL-6 may exacerbate disease. Given that IL-6 can amplify inflammation-induced injury to a variety of cells and tissues, it remains a valid therapeutic target (*31*), although it may be important to selectively target the pro-inflammatory effects of IL-6 while sparing its protective effects. The development of inhibitors that specifically target trans-signaling by inhibiting the docking of the IL-6–IL-6Rα complex to gp130 may offer a clinical advantage in selectively targeting the deleterious effects of

IL-6 without affecting the more beneficial effects, including the maintenance of protective Th17 cells.

Materials and Methods

Study Design

This study was designed to investigate whether ongoing IL-6 is required for Th17 function, and whether classical or trans signaling was more important for maintenance of Th17 cells. Experiments consisted of analyzing T cell populations in the inflamed intestines of immunodeficient recipients as part of two established T cell transfer models of colitis. All animals were bred and maintained in accordance with institutional animal care and use committee regulations. Littermate comparisons were used for all experiments where possible. Gender and aged matched male and female mice were used, and animals were randomly assigned into different groups. Group sizes were the minimum required to detect statistically significant differences based on previous experience. Experiments were not blinded to investigators, but histopathological samples were blinded prior to scoring. All experiments were replicated as presented in the figure legends.

Mice

The following mice were purchased from the Jackson Laboratories: C57BL/6.CD45.1, *Il6*$^{-/-}$, B6.FVB-Tg(*EIIa*^{Cre}), and *Rag1*$^{-/-}$. The generation of *Il17f*$^{Thy1.1/Thy1.1}$ reporter mice has been described previously (*19*). *Il17f*$^{Thy1.1}$ mice were crossed to B6.CD45.1 to create *Il17f*$^{Thy1.1}$(CD45.1). *Il6ra*^{flfl} mice were a gift from A. Drew (Univ. of Cincinnati) and were crossed with *EIIa*^{Cre} mice to generate *Il6ra*$^{-/-}$. Where indicated, crosses between *Il17f*$^{Thy1.1/Thy1.1}$ reporter mice and individual knockout mice were made in our facility to generate mice homozygous for *Il17f*$^{Thy1.1}$ and respective gene deletion alleles (eg. *Il6ra*$^{-/-}$). All mice were on a C57BL/6 background.

CD4 T cell preparation and culture

$CD4^+$ T cells were purified from pooled spleen and lymph nodes by Dynabeads Mouse CD4, followed by DETACHaBEAD Mouse CD4, according to the manufacturer's instructions (ThermoFisher). Naïve $CD4^+$ $CD62L^+$ $CD25^-$ T cells were obtained by FACS sorting. $CD4^+$ T cells were cultured at a ratio of 1:5 with irradiated splenic feeder cells (or, where noted, Dynabeads T-Activator CD3/CD28 beads (ThermoFisher)) for 7 d in RPMI containing 10% FBS, 100 IU/mL penicillin, 100 μg/mL streptomycin, 1 μM sodium pyruvate, 1x non-essential amino acids, 2.5 μM b-mercaptoethanol, and 2 μM L-glutamine (R10 medium). Cells were stimulated with 2.5 μg/mL anti-CD3 (clone 145-11), and for Th17 polarizations were supplemented with 2.5 ng/mL rhTGF-β1 (R&D systems), 10 ng/mL rmIL-6 (R&D systems) or 10 ng/mL hyper-IL-6 (S. Jones, Cardiff University), 10 μg/mL anti-IFN-γ (clone XMG1.2), and 10 ug/mL anti-IL-4 (clone 11B11). In restimulation cultures, viable T cells were recovered on day 7 of initial cultures and activated with fresh splenic feeders or CD3/CD28 activator beads, cytokines and antibody mixtures as indicated. Unless otherwise noted, rmIL-23 or rmIL-12 (R&D systems) were added at 20 ng/mL and 2.5 ng/ml respectively.

CD4 adoptive transfer model of colitis

CD4 cells were cultured under Th17 polarizing conditions for 7 d. Viable cells were recovered (Ficoll) and $Thy1.1^+$ cells were isolated by magnetic sorting (Miltenyi Biotec). A total of 4 x 10^5 $Thy1.1^+$ Th17 cells were injected i.p into age and sex matched *Rag1*$^{-/-}$ recipients. For co-transfer experiments, 2 x 10^5 each of WT and *Il6ra*$^{-/-}$ Th17 cells were transferred. For the naïve CD4 transfer model, $CD4^+$ $CD45RB^{Hi}$ cells were FACS sorted from pooled spleen and lymph nodes and a total of 4 x 10^5 cells were injected into age matched *Rag1*$^{-/-}$ recipients. Mice were monitored regularly for signs of disease and weighed weekly. At 4 or 8 weeks after transfer, mice were sacrificed and MLNs and colons were recovered. Colons were cut longitudinally, and small lengths of tissue were obtained from the proximal, middle and distal portions of the colon, fixed in 10% formalin, and

processed for histopathological analyses. Samples were scored by a pathologist in a blinded fashion as previously described (*86*).

Isolation of colonic lymphocytes

Lamina propria lymphocytes from the colon (CLP) were isolated as described previously(*86*). Briefly, colons were cut longitudinally, and were cut into 1 cm long strips. Tissues were washed in cold 1 x HBSS containing 2% (vol/vol) FBS plus 100 IU/mL penicillin and 100 μg/mL streptomycin. After being washed, tissues were digested at 37 C for 45 min with gentle stirring in R10 medium containing Collagenase D (100 U/mL) and DNase I (20 mg/mL) (Sigma). Lamina propria lymphocytes were purified on a 40%/75% (vol/vol) Percoll gradient by centrifugation for 20 min at 25 °C.

Flow cytometric analysis

Where indicated, $CD4^+$ cells were stimulated with PMA (50 ng/mL; Sigma) and Ionomycin (750 ng/mL; EMD Millipore) for 5 h in the presence of GolgiPlug (BD Biosciences). Intracellular staining was performed as previously described(*86*). LIVE/DEAD Fixable near-IR Dead Cell Stain (Invitrogen) was used to exclude dead cells. Staining of $CD4^+$ T cells was performed with antibodies to CD4 (RM4-5), IL-6Rα (D7715A7), IL-17A (TC11-18H10), TCR-β (H57-597) and Foxp3 (FJK-16s) from BD Biosciences, IFN-γ (XMG1.2), TCR-β (H57-597), gp130 (KGP130), and Thy1.1 (His51) from eBioscience, and Thy1.1 (OX-7) from Biolegend. For apoptosis analysis, Annexin V and Propidium Iodide staining was performed using an Annexin V Apoptosis Detectin Kit (eBioscience) according to manufacturer's instructions. Samples were acquired on an LSRII or Attune NxT flow cytometer and data were analyzed with FlowJo software (Tree Star).

Phospho-STAT staining

$CD4^+$ T cells from in vitro cultures or MLN cells from recipient *Rag1*$^{-/-}$ mice were rested for 4 h at 37 °C in RPMI, then stimulated for 15 min with 0.95 nM IL-6 or HDS. Cells were fixed for 15

min at 37 °C with 3% paraformaldehyde (PFA), then washed and permeabilized for 30 min at 4 °C with 90% methanol. Following two washes, cells were stained for 1 h at room temp with antibodies against CD4 (clone RM4-5), pSTAT3 (Y705; clone 4/P-STAT3) and pSTAT1 (Y701; clone 4a), all from BD Biosciences.

BrdU staining

Where noted, $CD4^+$ T cell recipient *Rag1*$^{-/-}$ mice were fed with 1 mg/mL Bromodeoxyuridine (BrdU; Sigma) in tap water with 1% sucrose (w/vol) for 7 d prior to sacrifice. At 1 and 4 weeks after transfer, $CD4^+$ cells from spleen, MLN and CLP were harvested and BrdU was detected using the BrdU Flow Kit (BD Biosciences) according to manufacturer's instructions. $CD4^+$ cells were co-stained with CD4 (RM4-5), LIVE/DEAD Fixable near-IR Dead Cell Stain, TCR-β (H57-597) and Ki67 (eBioscience, SolA15).

Measurement of IL-6, sIL6Rα, sgp130, and other analytes

Blood was collected from mice upon euthanasia, and serum obtained by centrifugation. For colon explant cultures, colon tissue was flushed, cut into three equal sections and then opened longitudinally. Individual tissue segments were minced and placed in 0.4 ml of R10 medium for 2 d, then supernatant collected by centrifugation. Cytokines and other analytes were measured by Milliplex assay (Millipore) following manufacturer's instructions.

Immunohistology

For immunostaining experiments, colons were fixed in 2% (vol/vol) PFA for 2 h at room temperature, washed in PBS, and then set overnight at 4 ºC in 20% (wt/vol) sucrose solution. Tissue was then rinsed in PBS, cut into equal segments, embedded in O.C.T. (Tissue-Tek), and snap frozen. Tissue sections (6-8 μm) were stained with biotinylated anti-CD45.1 (clone A20, eBioscience) followed by Streptavidin-Alexa Fluor 488 (Invitrogen), APC-conjugated anti-EpCAM1 (G8.8, eBioscience), and Alexa Fluor 594-conjugated anti-CD3 (17A2, eBioscience)

followed by donkey anti-goat IgG Alexa Fluor 594 to amplify the signal. Images were obtained using a Nikon A1R confocal microscope and processed with Nikon Elements software.

RNA-seq analysis

Adaptors were trimmed and aberrant reads were removed using TrimGalore (version 0.4.5). The quality controlled reads were mapped onto the mouse genome build GRCm38 (ENSEMBL.mus_musculus.release-75)(*87*) using STAR (version 2.5.3)(*88*). BAM files were sorted using SAMtools (version 0.1.18)(*89*), and reads were counted for each gene using HTSeq (version 0.7.2)(*90*). Differential expression analysis was performed using DESeq2 (version 1.18.1)(*91*) using R (version 3.4.3). Dispersion shrinkage of fold changes was performed with the ASHR algorithm (*92*). To prepare data for gene set enrichment analysis, results of differential gene expression analysis were ranked by signed p-value. Gene lists were ranked by p-value of Wald test multiplied by sign of fold-change and analyzed for enrichment of curated query gene sets using Fast Gene Set Enrichment Analysis (fgsea, version 1.4.0) with 1 million permutations. Gene set enrichment p-values of Normalized Enrichment Scores (NES) were corrected with the Benjamini-Hochberg procedure. When available, gene sets were made from reported results of transcriptome analysis. However, for many published data sets, only raw data were available, and gene sets were created using in-house scripts. Query gene sets were created from publicly available data. Raw data was obtained from the gene expression omnibus (*93*). Bulk RNA-seq data was analyzed as described above and gene sets were made by selecting the top 250 up and down regulated genes by p-value with a fold change of at least 1.5. Microarray data was analyzed using the limma R package (*94*). The functions model.matrix and lmFit were used to create and fit linear models, respectively. Due to the increased noise in microarray data, the top 125 up and down regulated genes were selected by p-value with a fold change of at least 1.5 to create gene sets. All query gene sets used are available in Supplemental Table 1.

The Jaccard indexes were calculated for each leading edge gene set versus all others by dividing the number of genes in the intersection by the number of genes in the union of each comparison. The resulting matrix underwent dimension reduction by using t-Stochastic Neighbor Embedding (t-SNE) as implemented in the R package Rtsne (version 0.13, with settings dim=2, perplexity=5, and max_iter = 50,000).

Gene set enrichment analysis

Gene set enrichment analysis was performed using software from the Broad Institute(*95*). A pre-ranked analysis was performed on a gene list ordered by signed p-value using Classic enrichment statistic, 10,000 permutations, and meandiv Normalization mode. Th17 and Th1 associated gene sets were created from publicly available microarrays (GEO GSE14308)(*57*). Limma (3.32.8) was used to calculate differential expression by comparing Th1 samples to Th17 samples. The top 250 genes by most significant adjusted p-value were separated by fold change. Those with a log2 transformed fold change greater than zero generated the Th1 gene set, those with fold changes less than zero generated the Th17 gene set. Hallmark gene sets were obtained from the MSigDB (*96*). Heatmaps were created using R 3.0.1 and the function heatmap.2 from the ggplot2 package (*97*).

Retrovirus production and CD4$^+$ T cell transduction

GFP and RORγt GFP retroviruses were produced by transfecting Platinum-E packaging cells (Cell Biolabs) with pMIG (Addgene #9044) or MIGR-RORgt (Addgene #24069) retroviral plasmids using Lipofectamine 2000 (ThermoFisher), and collecting supernatant 24 and 48 hours later.

To transduce Th17 cells, FACS-sorted naïve CD4$^+$ T cells from *Il17f*$^{Thy1.1}$ mice were cultured in R10 medium with Dynabeads Mouse T-activator CD3/CD28 beads (ThermoFisher) at a ratio of 5 beads per CD4$^+$ cell. After 24 hours, cells were spin infected with retrovirus containing media for 90 min (2500 rpm, 30 ºC). Cells were then washed with R10 medium and cultured for a further 4 d under Th17 polarizing conditions. For transfers, CD4$^+$ Thy1.1$^+$ GFP$^+$ cells were FACS sorted and injected i.p into age and sex matched *Rag1*$^{-/-}$ recipients.

Real-time PCR

Congenically marked CD4$^+$ TCR-β$^+$ cells were sorted from the CLP of *Rag1*$^{-/-}$ recipients. Total RNA was isolated using an miRNeasy Isolation kit (Qiagen) according to manufacturer's instructions. cDNA was synthesized with the iScript Reverse Transcription Supermix (BioRad), and real-time PCR was performed with SsoAdvanced Universal Probes Supermix or SsoAdvanced Universal SYBR Green Supermix (BioRad) for 35-40 cycles. Reactions were run in duplicate and normalized to *B2m*.

Statistical analysis

Statistical significance was calculated using Prism software (GraphPad). The nonparametric two-tailed Mann Whitney test or Kruskal Wallis test was used to determine significance for pathology data, all other data was analyzed using unpaired two-tailed Student's *t*-test or one-way ANOVA as appropriate. All P values ≤ 0.05 were considered significant.

References and Notes:

1. P. R. Mangan *et al*., Transforming growth factor-β induces development of the T_H17 lineage. *Nature*. **441**, 231–234 (2006).

2. C. T. Weaver, R. D. Hatton, P. R. Mangan, L. E. Harrington, IL-17 family cytokines and the expanding diversity of effector T cell lineages. *Annu. Rev. Immunol*. **25**, 821–852 (2007).

3. M. Veldhoen, R. J. Hocking, C. J. Atkins, R. M. Locksley, B. Stockinger, TGFβ in the Context of an inflammatory cytokine milieu supports de novo differentiation of IL-17-producing T cells. *Immunity*. **24**, 179–189 (2006).

4. E. Bettelli *et al*., Reciprocal developmental pathways for the generation of pathogenic

effector T_H17 and regulatory T cells. *Nature*. **441**, 235–238 (2006).

5. P. C. Heinrich *et al*., Principles of interleukin (IL)-6-type cytokine signalling and its regulation. *Biochem. J*. **374**, 1–20 (2003).

6. L. Durant *et al*., Diverse targets of the transcription factor STAT3 contribute to T cell pathogenicity and homeostasis. *Immunity*. **32**, 605–615 (2010).

7. X. O. Yang *et al*., STAT3 regulates cytokine-mediated generation of inflammatory helper T cells. *J. Biol. Chem*. **282**, 9358–9363 (2007).

8. L. Zhou *et al*., IL-6 programs T_H-17 cell differentiation by promoting sequential engagement of the IL-21 and IL-23 pathways. *Nat Immunol*. **8**, 967–974 (2007).

9. M. Ciofani *et al*., A validated regulatory network for Th17 cell specification. *Cell*. **151**, 289–303 (2012).

10. N. Yosef *et al*., Dynamic regulatory network controlling T_H17 cell differentiation. *Nature*. **496**, 461–468 (2013).

11. K. Ichiyama *et al*., Foxp3 inhibits RORγt-mediated IL-17A mRNA transcription through direct interaction with RORγt. *J. Biol. Chem*. **283**, 17003–17008 (2008).

12. I. I. Ivanov *et al*., The orphan nuclear receptor RORγt directs the differentiation program of proinflammatory IL-17$^+$ T helper cells. *Cell*. **126**, 1121–1133 (2006).

13. R. H. Duerr *et al*., A genome-wide association study identifies IL23R as an inflammatory bowel disease gene. *Science*. **314**, 1461–1463 (2006).

14. B. Khor, A. Gardet, R. J. Xavier, Genetics and pathogenesis of inflammatory bowel disease. *Nature*. **474**, 307–317 (2011).

15. P. P. Ahern *et al*., Interleukin-23 drives intestinal inflammation through direct activity on T cells. *Immunity*. **33**, 279–288 (2010).

16. R. P. Nair *et al*., Genome-wide scan reveals association of psoriasis with IL-23 and NF-κB pathways. *Nat Genet*. **41**, 199–204 (2009).

17. Australo-Anglo-American Spondyloarthritis Consortium (TASC) *et al*., Genome-wide association study of ankylosing spondylitis identifies non-MHC susceptibility loci. *Nat Genet*. **42**, 123–127 (2010).

18. C. O. Elson *et al*., Monoclonal anti–interleukin 23 reverses active colitis in a T cell–mediated model in mice. **132**, 2359–2370 (2007).

19. Y. K. Lee *et al*., Late developmental plasticity in the T helper 17 lineage. *Immunity*. **30**, 92–107 (2009).

20. M. J. McGeachy *et al*., The interleukin 23 receptor is essential for the terminal differentiation of interleukin 17–producing effector T helper cells in vivo. **10**, 314–324 (2009).

21. G. L. Stritesky, N. Yeh, M. H. Kaplan, IL-23 promotes maintenance but not commitment to the Th17 lineage. *J. Immunol*. **181**, 5948–5955 (2008).

22. C. L. Langrish *et al*., IL-23 drives a pathogenic T cell population that induces autoimmune inflammation. *J Exp Med*. **201**, 233–240 (2005).

23. K. Hirota *et al*., Fate mapping of IL-17-producing T cells in inflammatory responses. *Nat Immunol*. **12**, 255–263 (2011).

24. M. H. Lexberg *et al*., Th memory for interleukin-17 expression is stable in vivo. *Eur. J. Immunol*. **38**, 2654–2664 (2008).

25. P. J. Morrison *et al*., Th17-cell plasticity in *Helicobacter hepaticus*-induced intestinal inflammation. *Mucosal Immunol*. **6**, 1143–1156 (2013).

26. R. Mukasa *et al*., Epigenetic instability of cytokine and transcription factor gene loci underlies plasticity of the T helper 17 cell lineage. *Immunity*. **32**, 616–627 (2010).

27. Y. Lee *et al*., Induction and molecular signature of pathogenic T_H17 cells. *Nat Immunol*. **13**, 991–999 (2012).

28. T. Tanaka, M. Narazaki, T. Kishimoto, IL-6 in inflammation, immunity, and disease. *Cold Spring Harb Perspect Biol*. **6**, a016295–a016295 (2014).

29. J. Scheller, J. Grötzinger, S. R. John, Updating interleukin-6 classic- and trans-signaling. *Signal Transduction*. **6**, 240–259 (2006).

30. T. Hirano, Interleukin 6 and its receptor: ten years later. *Int. Rev. Immunol*. **16**, 249–284 (1998).

31. C. A. Hunter, S. A. Jones, IL-6 as a keystone cytokine in health and disease. **16**, 448–457 (2015).

32. M. J. Boulanger, D. C. Chow, E. E. Brevnova, K. C. Garcia, Hexameric structure and assembly of the interleukin-6/IL-6 alpha-receptor/gp130 complex. *Science*. **300**, 2101–2104 (2003).

33. M. Saito, K. Yoshida, M. Hibi, T. Taga, T. Kishimoto, Molecular cloning of a murine IL-6 receptor-associated signal transducer, gp130, and its regulated expression in vivo. *The Journal of Immunology*. **148**, 4066–4071 (1992).

34. J. V. Castell *et al*., Plasma clearance, organ distribution and target cells of interleukin-6/hepatocyte-stimulating factor in the rat. *Eur. J. Biochem*. **177**, 357–361 (1988).

35. H. H. Oberg, Differential expression of CD126 and CD130 mediates different STAT-3 phosphorylation in $CD4^{+}CD25^{-}$ and $CD25^{high}$ regulatory T cells. **18**, 555–563 (2006).

36. E. M. Briso, O. Dienz, M. Rincon, Cutting edge: soluble IL-6R is produced by IL-6R ectodomain shedding in activated CD4 T cells. *The Journal of Immunology*. **180**, 7102–7106 (2008).

37. J. Müllberg *et al*., A metalloprotease inhibitor blocks shedding of the IL-6 receptor and the p60 TNF receptor. *The Journal of Immunology*. **155**, 5198–5205 (1995).

38. J. Müllberg *et al*., The soluble interleukin-6 receptor is generated by shedding. *Eur. J. Immunol*. **23**, 473–480 (1993).

39. T. Jostock *et al*., Soluble gp130 is the natural inhibitor of soluble interleukin-6 receptor transsignaling responses. *Eur. J. Biochem*. **268**, 160–167 (2001).

40. G. Müller-Newen *et al*., Soluble IL-6 receptor potentiates the antagonistic activity of soluble gp130 on IL-6 responses. *The Journal of Immunology*. **161**, 6347–6355 (1998).

41. S. Heink *et al*., Trans-presentation of IL-6 by dendritic cells is required for the priming of pathogenic TH17 cells. *Nat Immunol*. **18**, 74–85 (2017).

42. P. C. Heinrich, J. V. Castell, T. Andus, Interleukin-6 and the acute phase response. *Biochem. J*. **265**, 621–636 (1990).

43. T. Hosokawa *et al*., Interleukin-6 and soluble interleukin-6 receptor in the colonic mucosa of inflammatory bowel disease. *J. Gastroenterol. Hepatol*. **14**, 987–996 (1999).

44. R. Atreya *et al*., Blockade of interleukin 6 trans signaling suppresses T-cell resistance against apoptosis in chronic intestinal inflammation: evidence in crohn disease and experimental colitis in vivo. *Nat Med*. **6**, 583–588 (2000).

45. S. M. Hurst *et al*., Il-6 and its soluble receptor orchestrate a temporal switch in the pattern of leukocyte recruitment seen during acute inflammation. *Immunity*. **14**, 705–714 (2001).

46. G. W. Jones *et al*., Loss of CD4+ T cell IL-6R expression during inflammation underlines a role for IL-6 transsignaling in the local maintenance of Th17 cells. *The Journal of Immunology*. **184**, 2130–2139 (2010).

47. F. Powrie, M. W. Leach, S. Mauze, L. B. Caddle, R. L. Coffman, Phenotypically distinct subsets of CD4+ T cells induce or protect from chronic intestinal inflammation in C. B-17 scid mice. *International Immunology*. **5**, 1461–1471 (1993).

48. M. Leppkes *et al*., RORγ-expressing Th17 cells induce murine chronic intestinal inflammation via redundant effects of IL-17A and IL-17F. *Gastroenterology*. **136**, 257–267 (2009).

49. S. A. Nish *et al*., T cell-intrinsic role of IL-6 signaling in primary and memory responses. *eLife*. **3**, e01949–19 (2014).

50. T. Feng, L. Wang, T. R. Schoeb, C. O. Elson, Y. Cong, Microbiota innate stimulation is a prerequisite for T cell spontaneous proliferation and induction of experimental colitis. *J Exp Med*. **207**, 1321–1332 (2010).

51. M. Fujimoto *et al*., Interleukin-6 blockade suppresses autoimmune arthritis in mice by the inhibition of inflammatory Th17 responses. *Arthritis Rheum*. **58**, 3710–3719 (2008).

52. T. K. Teague, P. Marrack, J. W. Kappler, A. T. Vella, IL-6 rescues resting mouse T cells from apoptosis. *The Journal of Immunology*. **158**, 5791–5796 (1997).

53. U. A. Betz, W. Müller, Regulated expression of gp130 and IL-6 receptor alpha chain in T cell maturation and activation. *International Immunology*. **10**, 1175–1184 (1998).

54. T. K. Teague *et al*., Activation-induced inhibition of interleukin 6-mediated T cell survival and signal transducer and activator of transcription 1 signaling. **191**, 915–926 (2000).

55. G. Perona-Wright *et al*., Persistent loss of IL-27 responsiveness in $CD8^+$ memory T cells abrogates IL-10 expression in a recall response. *Proc. Natl. Acad. Sci. U.S.A.* **109**, 18535–18540 (2012).

56. X. J. Wang *et al*., gp130, the cytokine common signal-transducer of interleukin-6 cytokine family, is downregulated in T cells in vivo by interleukin-6. *Blood*. **91**, 3308–3314 (1998).

57. G. Wei *et al*., Global mapping of H3K4me3 and H3K27me3 reveals specificity and plasticity in lineage fate determination of differentiating $CD4^+$ T cells. *Immunity*. **30**, 155–167 (2009).

58. C. Schiering *et al*., The alarmin IL-33 promotes regulatory T-cell function in the intestine. *Nature*. **513**, 564–568 (2014).

59. L. E. Harrington *et al*., Interleukin 17–producing $CD4^+$ effector T cells develop via a lineage distinct from the T helper type 1 and 2 lineages. *Nat Immunol*. **6**, 1123–1132 (2005).

60. B. Guo, E. Y. Chang, G. Cheng, The type I IFN induction pathway constrains Th17-mediated autoimmune inflammation in mice. *J. Clin. Invest*. **118**, 1680–1690 (2008).

61. V. Lazarevic *et al*., T-bet represses T_H17 differentiation by preventing Runx1-mediated activation of the gene encoding RORγt. *Nat Immunol*. **12**, 96–104 (2011).

62. C. T. Weaver, L. E. Harrington, P. R. Mangan, M. Gavrieli, K. M. Murphy, Th17: an effector CD4 T cell lineage with regulatory T cell ties. *Immunity*. **24**, 677–688 (2006).

63. X.-P. Yang *et al*., Opposing regulation of the locus encoding IL-17 through direct,

reciprocal actions of STAT3 and STAT5. *Nat Immunol*. **12**, 247–254 (2011).

64. A. Laurence *et al*., Interleukin-2 signaling via STAT5 constrains T helper 17 cell generation. *Immunity*. **26**, 371–381 (2007).

65. K. M. Murphy, B. Stockinger, Effector T cell plasticity: flexibility in the face of changing circumstances. *Nat Immunol*. **11**, 674–680 (2010).

66. K. M. Murphy, S. L. Reiner, The lineage decisions of helper T cells. *Nature Reviews Immunology*. **2**, 933–944 (2002).

67. K. Hirahara *et al*., Asymmetric Action of STAT Transcription Factors Drives Transcriptional Outputs and Cytokine Specificity. *Immunity*. **42**, 877–889 (2015).

68. T. Korn *et al*., IL-21 initiates an alternative pathway to induce proinflammatory T(H)17 cells. *Nature*. **448**, 484–487 (2007).

69. T. R. Malek, The biology of interleukin-2. *Annu. Rev. Immunol*. **26**, 453–479 (2008).

70. C. L. Maynard, C. O. Elson, R. D. Hatton, C. T. Weaver, Reciprocal interactions of the intestinal microbiota and immune system. *Nature*. **489**, 231–241 (2012).

71. F. Powrie, R. Correa-Oliveira, S. Mauze, R. L. Coffman, Regulatory interactions between $CD45RB^{high}$ and $CD45RB^{low}$ $CD4^{+}$ T cells are important for the balance between protective and pathogenic cell-mediated immunity. *J Exp Med*. **179**, 589–600 (1994).

72. S. Hue *et al*., Interleukin-23 drives innate and T cell–mediated intestinal inflammation. *J Exp Med*. **203**, 2473–2483 (2006).

73. S. N. Harbour, C. L. Maynard, C. L. Zindl, T. R. Schoeb, C. T. Weaver, Th17 cells give rise to Th1 cells that are required for the pathogenesis of colitis. *Proc. Natl. Acad. Sci. U.S.A*. **112**, 7061–7066 (2015).

74. V. Matthews *et al*., Cellular cholesterol depletion triggers shedding of the human interleukin-6 receptor by ADAM10 and ADAM17 (TACE). *J. Biol. Chem.* **278**, 38829–38839 (2003).

75. C. Garbers *et al*., Species specificity of ADAM10 and ADAM17 proteins in interleukin-6 (IL-6) trans-signaling and novel role of ADAM10 in inducible IL-6 receptor shedding. *J. Biol. Chem.* **286**, 14804–14811 (2011).

76. W. Liao, J.-X. Lin, L. Wang, P. Li, W. J. Leonard, Modulation of cytokine receptors by IL-2 broadly regulates differentiation into helper T cell lineages. *Nat Immunol.* **12**, 551–559 (2011).

77. S. Eyre *et al*., High-density genetic mapping identifies new susceptibility loci for rheumatoid arthritis. *Nat Genet.* **44**, 1336–1340 (2012).

78. C. A. Parisinos *et al*., Variation in interleukin 6 receptor gene associates with risk of Crohn's disease and ulcerative colitis. *YGAST*, 1–17 (2018).

79. C. Garbers *et al*., The interleukin-6 receptor Asp358Ala single nucleotide polymorphism rs2228145 confers increased proteolytic conversion rates by ADAM proteases. *Biochim. Biophys. Acta.* **1842**, 1485–1494 (2014).

80. P. Emery *et al*., IL-6 receptor inhibition with tocilizumab improves treatment outcomes in patients with rheumatoid arthritis refractory to anti-tumour necrosis factor biologicals: results from a 24-week multicentre randomised placebo-controlled trial. *Ann Rheum Dis.* **67**, 1516–1523 (2008).

81. D. Khanna *et al*., Safety and efficacy of subcutaneous tocilizumab in systemic sclerosis: results from the open-label period of a phase II randomised controlled trial (faSScinate). *Ann Rheum Dis.* **77**, 212–220 (2018).

82. S. Yokota *et al*., Efficacy and safety of tocilizumab in patients with systemic-onset juvenile idiopathic arthritis: a randomised, double-blind, placebo-controlled, withdrawal phase III trial. *Lancet*. **371**, 998–1006 (2008).

83. H. Ito *et al*., A pilot randomized trial of a human anti-interleukin-6 receptor monoclonal antibody in active Crohn's disease. *YGAST*. **126**, 989–96– discussion 947 (2004).

84. W. O'Connor *et al*., A protective function for interleukin 17A in T cell-mediated intestinal inflammation. *Nat Immunol*. **10**, 603–609 (2009).

85. S. Rose-John, IL-6 Trans-Signaling via the Soluble IL-6 Receptor: Importance for the Pro-Inflammatory Activities of IL-6. *Int. J. Biol. Sci*. **8**, 1237–1247 (2012).

86. C. L. Maynard *et al*., Regulatory T cells expressing interleukin 10 develop from Foxp3^{+} and Foxp3^{-} precursor cells in the absence of interleukin 10. *Nat Immunol*. **8**, 931–941 (2007).

87. T. Hubbard *et al*., The Ensembl genome database project. *Nucleic Acids Res*. **30**, 38–41 (2002).

88. A. Dobin *et al*., STAR: ultrafast universal RNA-seq aligner. *Bioinformatics*. **29**, 15–21 (2013).

89. H. Li *et al*., The Sequence Alignment/Map format and SAMtools. *Bioinformatics*. **25**, 2078–2079 (2009).

90. S. Anders, P. T. Pyl, W. Huber, HTSeq--a Python framework to work with high-throughput sequencing data. *Bioinformatics*. **31**, 166–169 (2015).

91. M. I. Love, W. Huber, S. Anders, Moderated estimation of fold change and dispersion for RNA-seq data with DESeq2. *Genome Biol*. **15**, 550 (2014).

92. M. Stephens, False discovery rates: a new deal. *Biostatistics*. **18**, 275–294 (2017).

93. R. Edgar, M. Domrachev, A. E. Lash, Gene Expression Omnibus: NCBI gene expression and hybridization array data repository. *Nucleic Acids Res*. **30**, 207–210 (2002).

94. M. E. Ritchie *et al*., limma powers differential expression analyses for RNA-sequencing and microarray studies. *Nucleic Acids Res*. **43**, e47 (2015).

95. A. Subramanian *et al*., Gene set enrichment analysis: a knowledge-based approach for interpreting genome-wide expression profiles. *Proceedings of the National Academy of Sciences*. **102**, 15545–15550 (2005).

96. A. Liberzon *et al*., The Molecular Signatures Database (MSigDB) hallmark gene set collection. *Cell Syst*. **1**, 417–425 (2015).

97. H. Wickham, ggplot2: Elegant Graphics for Data Analysis Springer-Verlag. *New York* (2009).

Acknowledgments:

The authors are grateful to members of the Weaver laboratory for helpful comments and suggestions. We thank D. O'Quinn, D.J. Wright and H. Turner for technical assistance. We also thank A. Drew (University of Cincinnati) for the provision of *Il6ra*$^{fl/fl}$ mice. We gratefully acknowledge the UAB Comparative Pathology laboratory for histology, the UAB High Resolution Imaging Facility (NIH P30 AR048311) for confocal microscopy images, the UAB Epitope Recognition and Immunoreagent Core Facility (NIH P30 AR048311) for antibody preparations, and the CFAR Basic and Translational Sciences Core Facility (NIH P30 AI27667) for FACS sorting.

Funding

This work was supported by NIH R01 DK093015, NIH R01 DK103744, grants from the Crohns and Colitis Foundation of America, and UAB Institutional Funds to CTW, as well as Versus Arthritis (Ref 20770, 19796) and Wellcome Trust (Ref 079044) to GWJ and SAJ.

Author contributions

SNH and CTW designed the research strategy and wrote the manuscript. SNH, DDT, CLZ, RDH performed experiments. SNH, SJW, TRS and CTW analyzed experiments. SAJ and GWJ provided key reagents and made helpful suggestions.

Data and materials availability

Gene expression data have been deposited in the NCBI Gene Expression Omnibus with the accession number GSE115141.

Figures

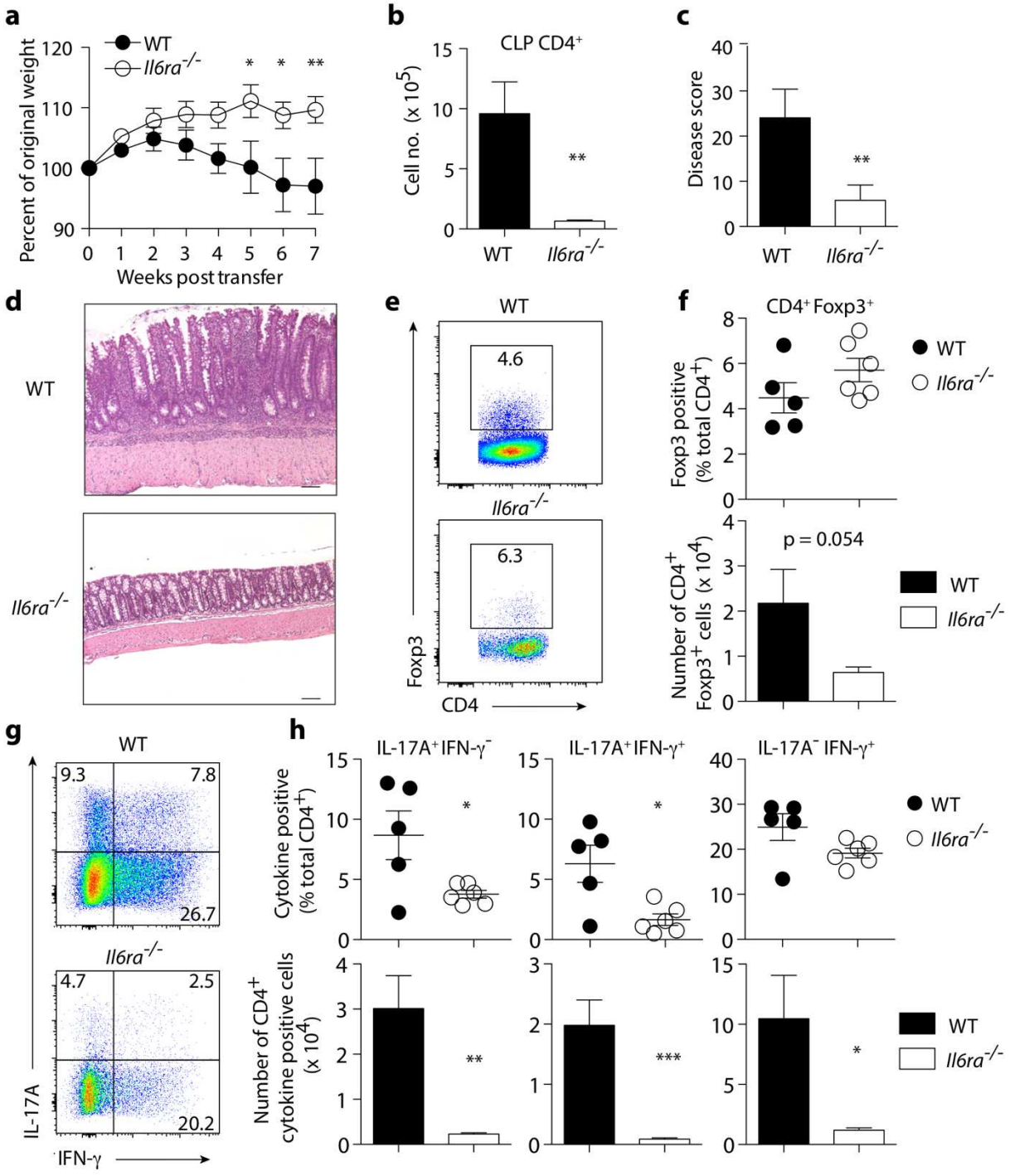

Fig. 1. Naïve CD4+ T cells require IL-6 for development and colitis pathogenesis. FACS sorted CD4+ CD45RB^{Hi} T cells isolated from WT and *Il6ra*$^{-/-}$ mice were transferred into *Rag1*$^{-/-}$ recipients (4 x 10^5/mouse)(n = 5 per group) and analyzed for colitis 8 weeks after transfer. (**A**) Weight loss

expressed as a percentage of starting weight (mean ± SEM). * $P < 0.05$, ** $P < 0.01$. (**B**) Total numbers of $CD4^+$ T cells recovered from the CLP of colitic mice (mean + SEM). ** $P = 0.0044$. (**C**) Histological scores (mean + SEM). ** $P = 0.005$ (**E**) Representative H&E stained sections of colon from recipients of WT (upper panel) or *Il6ra*$^{-/-}$ CD4+ T cells. H&E stain; original magnification 10x; scale bars 100 μm (**E**) Representative FACS plots showing Foxp3 expression in CLP $CD4^+$ T cells *ex vivo* from WT or *Il6ra*$^{-/-}$ recipients after development of colitis. (**F**) Relative frequencies (upper) and total numbers (lower) of $Foxp3^+$ $CD4^+$ T cells from the CLP (mean ± SEM). $P = 0.1724$ (upper), $P = 0.054$ (lower) (**G**) Representative FACS plots showing IL-17A and IFN-γ in CLP $CD4^+$ T cells *ex vivo* after development of colitis. (**H**) Relative frequencies (upper) and total numbers (lower) of IL-$17A^+$, IL-$17A^+$IFN-γ^+, and IFN-γ^+CD4^+ T cells in the CLP of colitic mice (mean ± SEM). * $P = 0.0268$, * $P = 0.0121$, $P = 0.0803$ (upper IL-$17A^+$, IL-$17A^+$IFN-γ^+, and IFN-γ^+CD4^+ T cells); ** $P = 0.0023$, *** $P = 0.0008$, * $P = 0.0191$ (lower IL-$17A^+$, IL-$17A^+$IFN-γ^+, and IFN-γ^+CD4^+ T cells) Data are representative of at least three independent experiments (**A**, **D**-**H**; n = 5 per group), or pooled from two independent experiments (**B**, **C**; n = 10 per group). *P* values; two-way ANOVA with Bonferroni post-test (**a**) or unpaired two-tailed Student's *t*-test (**B**-**C**, **F**, **H**).

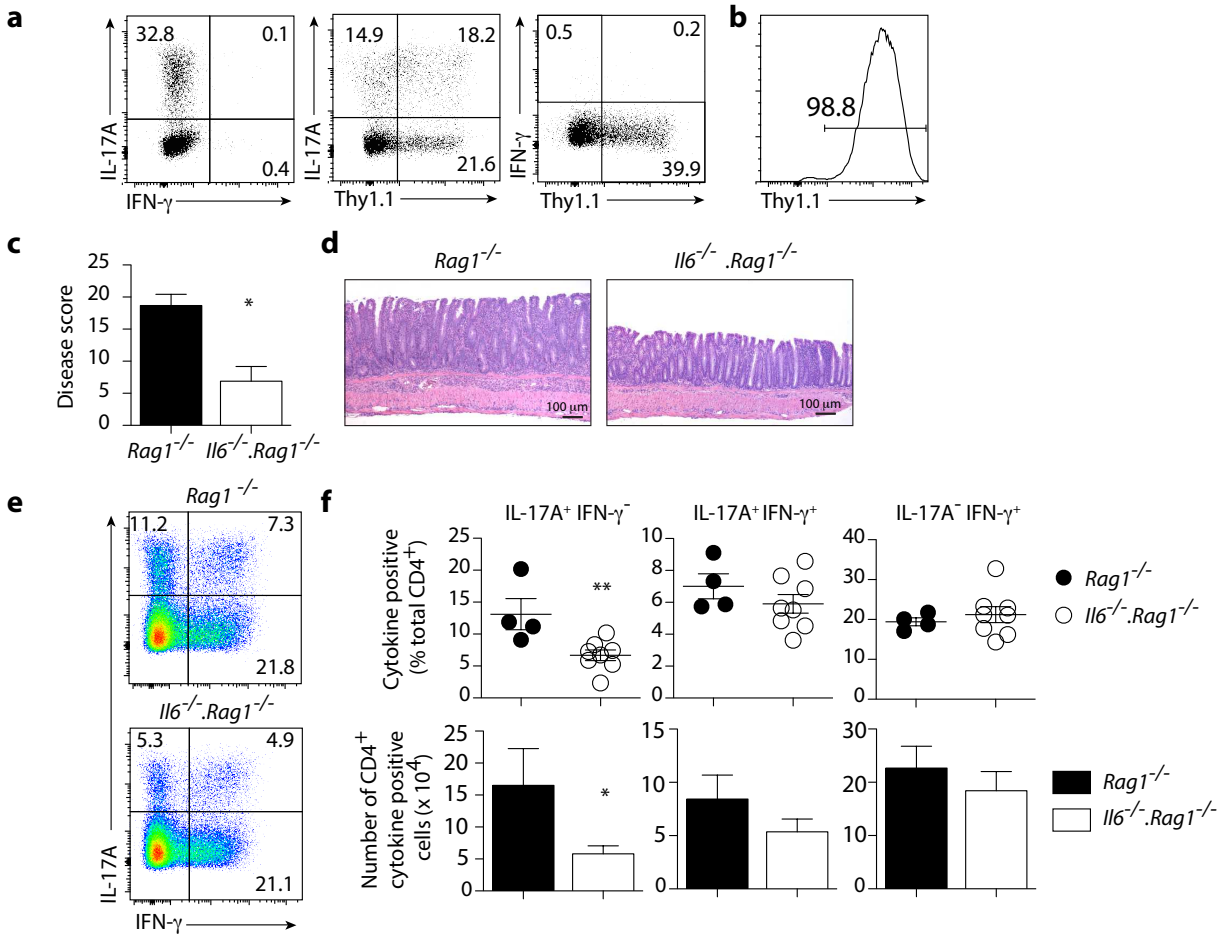

Fig. 2. Maintenance and pathogenesis of Th17 cells is dependent on persistent IL-6 signaling. CD4+ T cells from *Il17f*$^{thy1.1}$ mice were cultured with splenic feeder cells under Th17 polarizing conditions (2.5 µg/ml anti-CD3, 2.5 ng/ml TGF-β, 10 ng/ml IL-6, 10 µg/ml anti-IFN-γ, 10 µg/ml anti-IL-4) for 7 d. (**A**) Expression of IL-17A, IFN-γ and Thy1.1 in a fraction of *in vitro* cultured CD4+ T cells after PMA/Ionomycin stimulation for 5 h in the presence of monensin. (**B**) Thy1.1 expression in CD4+ T cells after purification of Thy1.1+ (IL-17F+) Th17 cells. 4 x 10^5 cells Th17 cells per mouse were transferred into *Rag1*$^{-/-}$ (n = 4) or *Il6*$^{-/-}$ *Rag1*$^{-/-}$ (n = 8) mice. Four weeks after transfer, mice were analyzed for development of colitis. (**C**) Histological scores (mean + SEM). * $P = 0.0264$. (**D**) Representative H&E stained sections of colon from *Rag1*$^{-/-}$ (left) or *Il6*$^{-/-}$. *Rag1*$^{-/-}$ (right) recipients of WT Th17 cells. H&E stain; original magnification 10x; scale bars 100 µm. (**E**) Representative FACS plots showing IL-17A and IFN-γ in CLP CD4+ T cells *ex vivo*. (**F**) Relative frequencies (upper) and total numbers (lower) of IL-17A+, IL-17A+ IFN-γ+, and IFN-γ+

$CD4^+$ T cells in the CLP of colitic mice (mean ± SEM). ** $P = 0.0099$, * $P = 0.0302$. Data are representative of at least two independent experiments. *P* values; unpaired two-tailed Mann-Whitney test (**C**) or unpaired two-tailed Student's *t*-test (**F**).

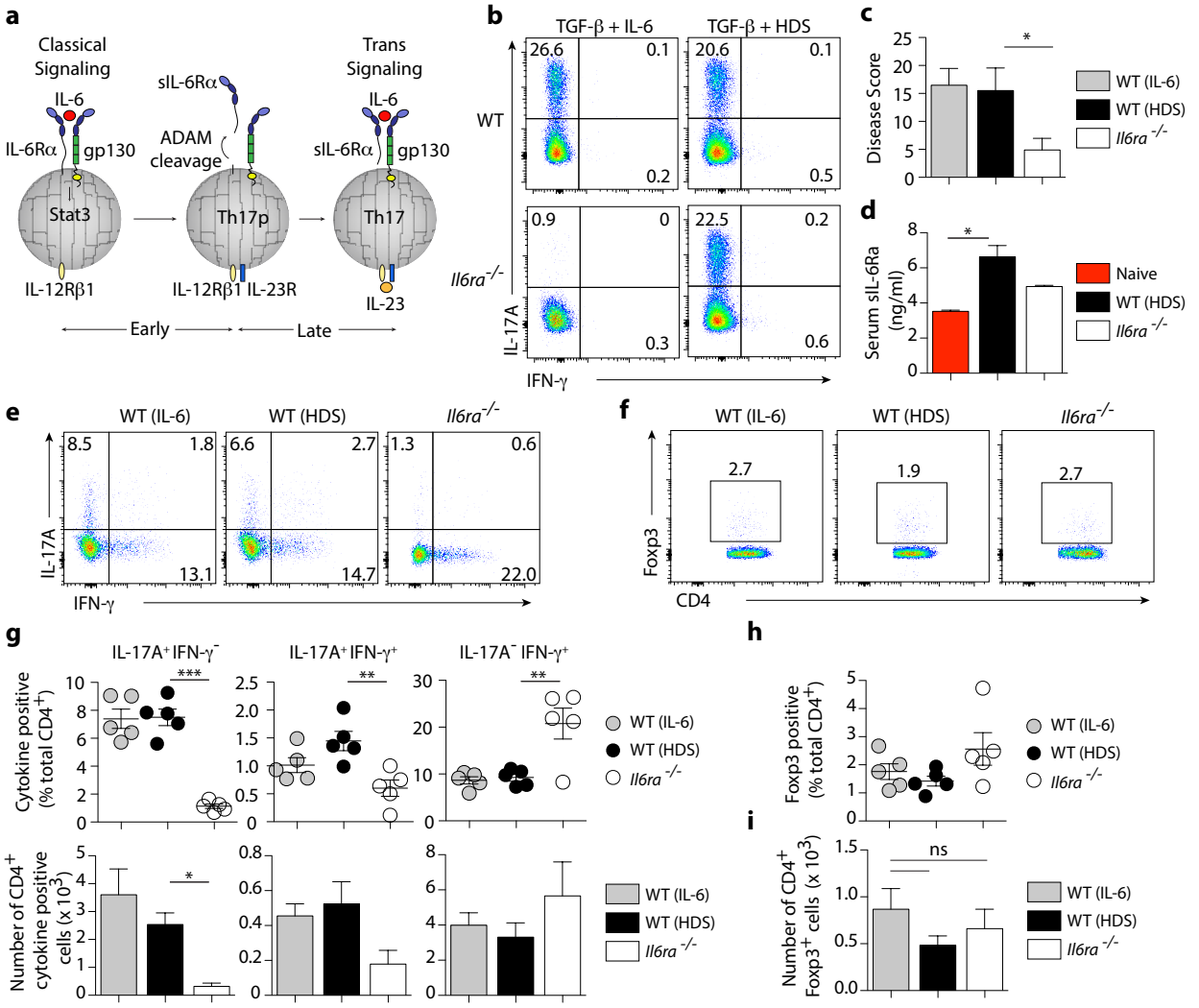

Fig. 3. Classic IL-6 signaling is required for maintenance of pathogenic Th17 cells. (**A**) Model of classic vs. trans IL-6 signaling in Th17 development. Early Th17 development is mediated by classic IL-6 signaling involving membrane IL-6Rα associating with gp130 (left). After activation, IL-6Rα is cleaved by ADAM proteases (middle), and late development is believed to be mediated by trans-signaling (right), where shed soluble IL-6Rα (sIL-6Rα) complexes with IL-6 and binds gp130 to induce signaling. (**B**) CD4+ T cells from *Il17f*$^{thy1.1}$ (WT) and *Il6ra*$^{-/-}$.*Il17f*$^{thy1.1}$ *(Il6ra*$^{-/-}$*)* were cultured with irradiated splenic feeder cells under Th17 polarizing conditions (2.5 μg/ml anti-CD3, 2.5 ng/ml TGF-β, 10 μg/ml anti-IFN-γ, 10 μg/ml anti-IL-4) for 7 d with 10 ng/ml IL-6 or 10 ng/ml recombinant IL-6-sIL6Ra (HDS). A fraction of cells was analyzed for expression of CD4 and intracellular IL-17A and IFN-γ after PMA/Ionomycin stimulation for 5 hr in the presence of

monensin. FACS plots are gated on $CD4^+$ cells. (**C**) WT (IL-6), WT (HDS) and *Il6ra*$^{-/-}$ $Thy1.1^+$ Th17 cells obtained in (**B**) were transferred into *Rag1*$^{-/-}$ mice (4 x 10^5/mouse). Histological scores were analyzed four weeks after transfer (mean + SEM)(WT (IL-6) n = 8, WT (HDS) n = 13, *Il6ra*$^{-/-}$ n = 12). * $P = 0.0305$. (**D**) Serum sIL-6Rα levels from naïve *Rag1*$^{-/-}$ mice as well as colitic recipients of WT (hIL-6) and *Il6ra*$^{-/-}$ Th17 cells at 4 weeks post transfer (n = 5 per group) were quantified by Milliplex assay (mean + SEM). * $P < 0.05$. (**E**) Representative FACS plots showing IL-17A and IFN-γ in CLP $CD4^+$ T cells *ex vivo*. (**F**) Representative FACS plots showing Foxp3 in CLP $CD4^+$ T cells *ex vivo*. (**G**) Relative frequencies (upper) and total numbers (lower) of IL-$17A^+$, IL-$17A^+$ IFN-γ^+, and IFN-γ^+ $CD4^+$ T cells in the CLP of colitic mice (mean ± SEM)(n = 5 per group). (**H**) Relative frequencies and (**I**) total numbers of $CD4^+$ $Foxp3^+$ T cells in the CLP of colitic mice (mean +/- SEM). Data are pooled from (**C**) or representative of (**E** – **I**) three independent experiments. *P* values; non parametric Kruskal-Wallis with Dunn's post comparison test (**C**), one-way ANOVA with Bonferroni post test (**D**) or Tukey's Multiple Comparison test (**G** – **I**).

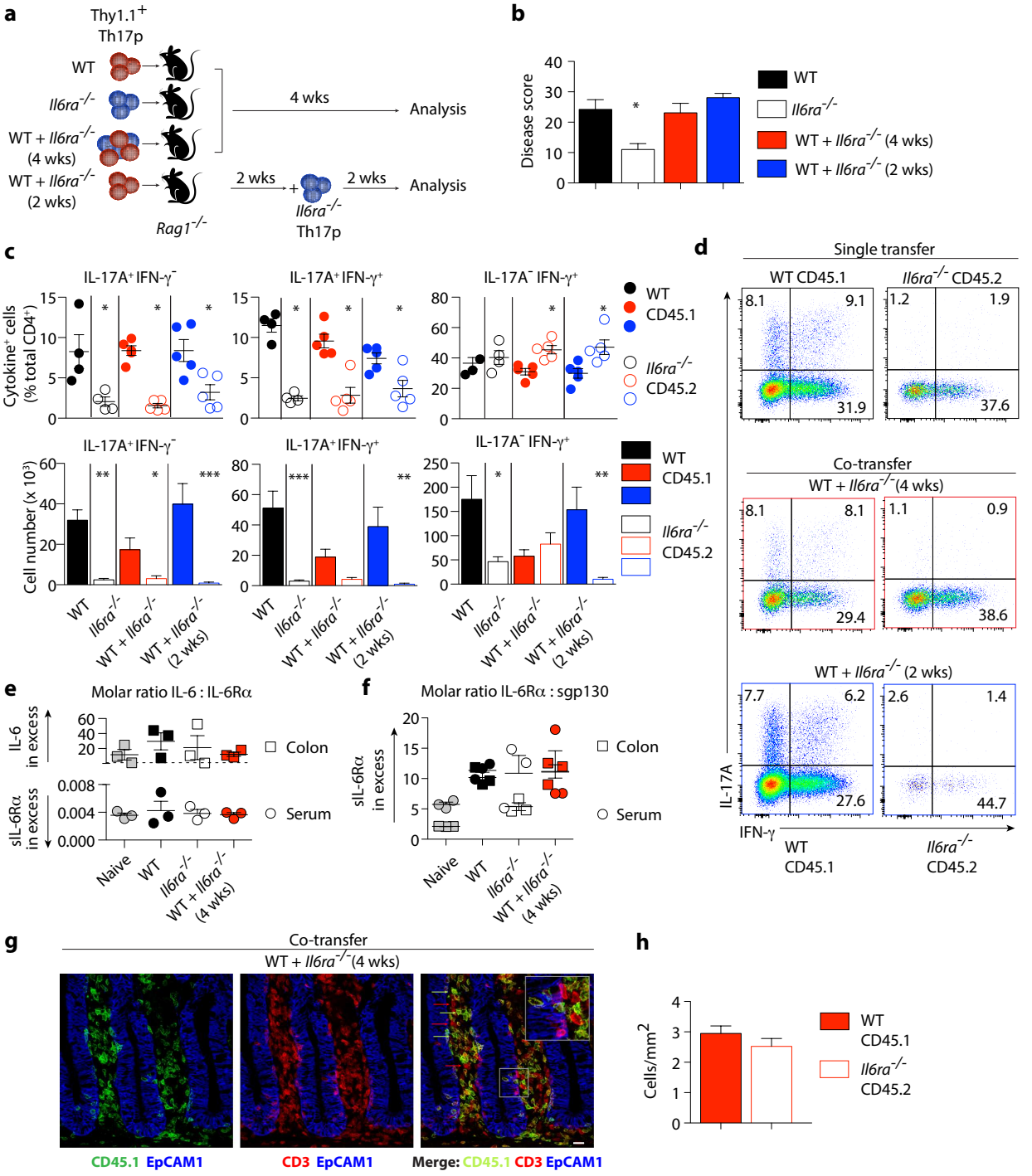

Fig. 4. Loss of Th17 phenotype in IL-6Rα-deficient Th17 cells is not rescued by co-transfer of WT Th17 cells. (**A**) Experimental schematic. CD4+ T cells from *Il17f*$^{thy1.1}$CD45.1 (WT) and *Il6ra*$^{-/-}$*Il17f*$^{thy1.1}$ (*Il6ra*$^{-/-}$) were cultured with irradiated splenic feeder cells under Th17 polarizing conditions for 7 d with 10 ng/ml HDS. Thy1.1+ Th17 cells were transferred separately (4 x

10^5/mouse) or together (2 x 10^5 each/mouse) into *Rag1*$^{-/-}$ recipients (WT n = 4, *Il6ra*$^{-/-}$ n = 4, WT + *Il6ra*$^{-/-}$ n = 5, WT + *Il6ra*$^{-/-}$ (2 wks) n = 5). (**B**) Histological scores were analyzed four weeks after transfer (mean + SEM). * $P < 0.05$ (**C**) Relative frequencies (upper) and total numbers (lower) of IL-17A$^+$, IL-17A$^+$ IFN-γ^+, and IFN-γ^+CD4$^+$ T cells in the CLP of colitic mice (mean ± SEM). * $P < 0.05$, ** $P < 0.01$, *** $P < 0.001$. (**D**) Representative FACS plots showing IL-17A and IFN-γ in CLP CD4$^+$ T cells from recipients of single or co-transfers *ex vivo* after development of colitis. (**E-F**) Levels of sIL-6Rα, sgp130 and IL-6 in colon explants and serum of naïve *Rag1*$^{-/-}$ mice as well as colitic recipients of single or co-transfer Th17 cells were quantified by Milliplex assay. Molar ratio of IL-6–IL-6Rα (**E**) and IL-6Rα–sgp130 (**F**) in colon explants (squares) and serum (circles) from colitic mice are shown. (**G**) Colon tissue from WT + *Il6ra*$^{-/-}$ Th17 co-transfers were stained with anti-EpCAM1 (blue), anti-CD45.1 (green) and anti-CD3 (red). Left panel shows anti-CD45.1 (WT), middle panel shows anti-CD3 (total T cells), right panel shows merged image (red arrows, *Il6ra*$^{-/-}$ CD4$^+$ T cells ; green arrows, WT CD4$^+$ T cells). Scale bars 20 μm. (**H**) Quantification of WT and *Il6ra*$^{-/-}$ CD4$^+$ T cells from (**G**). Data are representative of three independent experiments. P values; non parametric Kruskal-Wallis with Dunn's post comparison test (**B**), one-way ANOVA with Bonferroni post test (**C**).

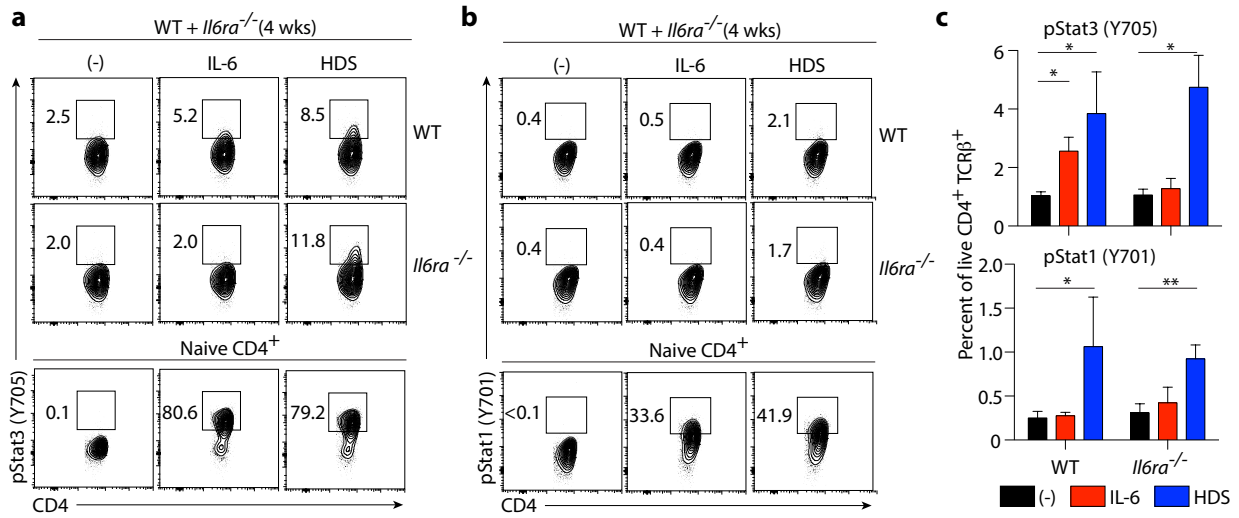

Fig. 5. IL-6Rα-deficient Th17 cells are responsive to trans-signaling *ex vivo*. Thy1.1$^+$ Th17 cells from *Il17f*$^{Thy1.1}$CD45.1(WT) and *Il6ra*$^{-/-}$*.Il17f*$^{Thy1.1}$ *(Il6ra*$^{-/-}$*)* were adoptively transferred together (2 x 10^5 each/mouse) into *Rag1*$^{-/-}$ recipients (n = 4 mice). Four weeks after transfer, CD4$^+$ cells from the MLN of recipient mice or naïve CD4$^+$ cells from the MLN of WT mice were stimulated with equimolar concentrations of IL-6 or HDS (0.95nM) for 15 min. (**A**) Representative FACS plots showing pSTAT3 (Y705) in MLN CD4$^+$ T cells from naïve or colitic mice. (**B**) Representative FACS plots showing pSTAT1 (Y701) in MLN CD4$^+$ T cells from naïve or colitic mice. (**C**). Relative frequencies of pSTAT3$^+$ (upper) and pSTAT1$^+$ CD4$^+$ T cells (lower) in the MLN of colitic mice (mean + SEM). * $P < 0.05$, ** $P < 0.01$. Data are representative of two independent experiments. *P* values; two-way ANOVA with Bonferroni post-test (**C**).

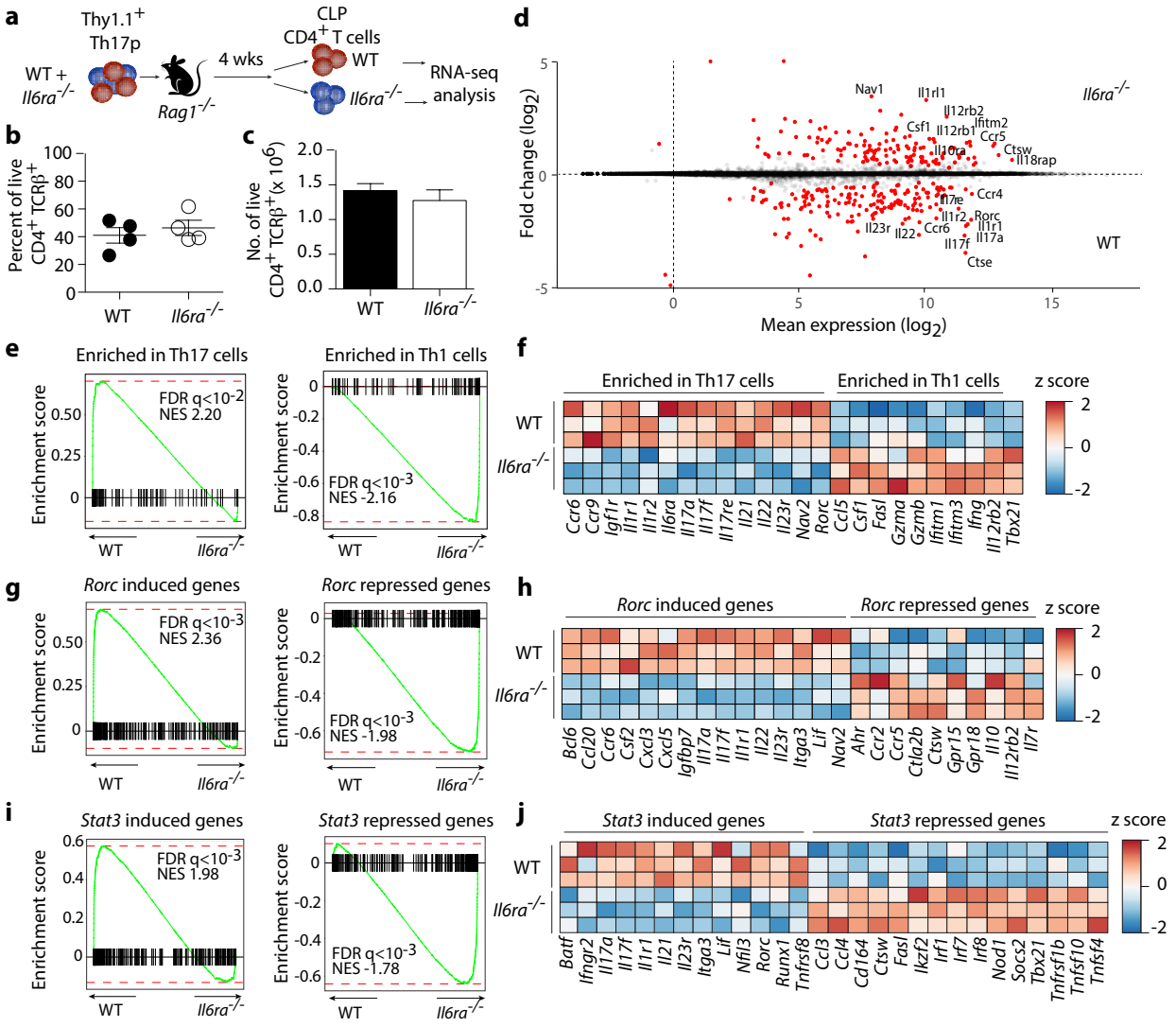

Fig. 6. IL-6 is required to maintain a Th17 gene program *in vivo*. (**A**) Experimental schematic. Thy1.1+ Th17 cells from *Il17f*$^{Thy1.1}$CD45.1 (WT) and *Il6ra*$^{-/-}$*Il17f*$^{Thy1.1}$ (*Il6ra*$^{-/-}$) were adoptively transferred together (2 x 10^5 each/mouse) into *Rag1*$^{-/-}$ recipients (n = 4). Four weeks after transfer, congenically marked CD4+ cells from the CLP of recipient mice were isolated and gene expression was assessed by RNA-seq. (**B**) Recovery of CLP CD4+ cells from *Rag1*$^{-/-}$ recipients of WT and *Il6ra*$^{-/-}$ Th17 cells (mean ± SEM). (**C**) Total number of CLP CD4+ T cells recovered from *Rag1*$^{-/-}$ recipients (mean + SEM). (**D**) MA plot displaying differentially expressed genes in WT (lower) and *Il6ra*$^{-/-}$ (upper) CD4+ T cells *ex vivo*. Red circles indicate genes with false discovery rate (FDR) <0.05. (**E**) Barcode plots of gene set enrichment results obtained using a set of genes previously

reported to be differentially expressed between Th17 cells (left) or Th1 cells (right) (data from GSE 14308) (NES, normalized enrichment score). (**F**) Expression of representative Th1 and Th17 cell associated genes identified by gene set enrichment in (**E**) are depicted by heat map with z-scored expression values. (**G**) Barcode plots of gene set enrichment results obtained using a set of genes previously reported to be regulated by *Rorc* in Th17 cells (GSE 40918). (**H**) Expression of representative genes identified by gene set enrichment in (**G**) are depicted by heat map with z-scored expression values. (**I**) Barcode plots of gene set enrichment results obtained using a set of genes previously reported to be regulated by *Stat3* in Th17 cells (GSE 40918) (**J**). Expression of representative genes identified by gene set enrichment in (**I**) are depicted by heat map with z-scored expression values. Data are from two independent experiments.

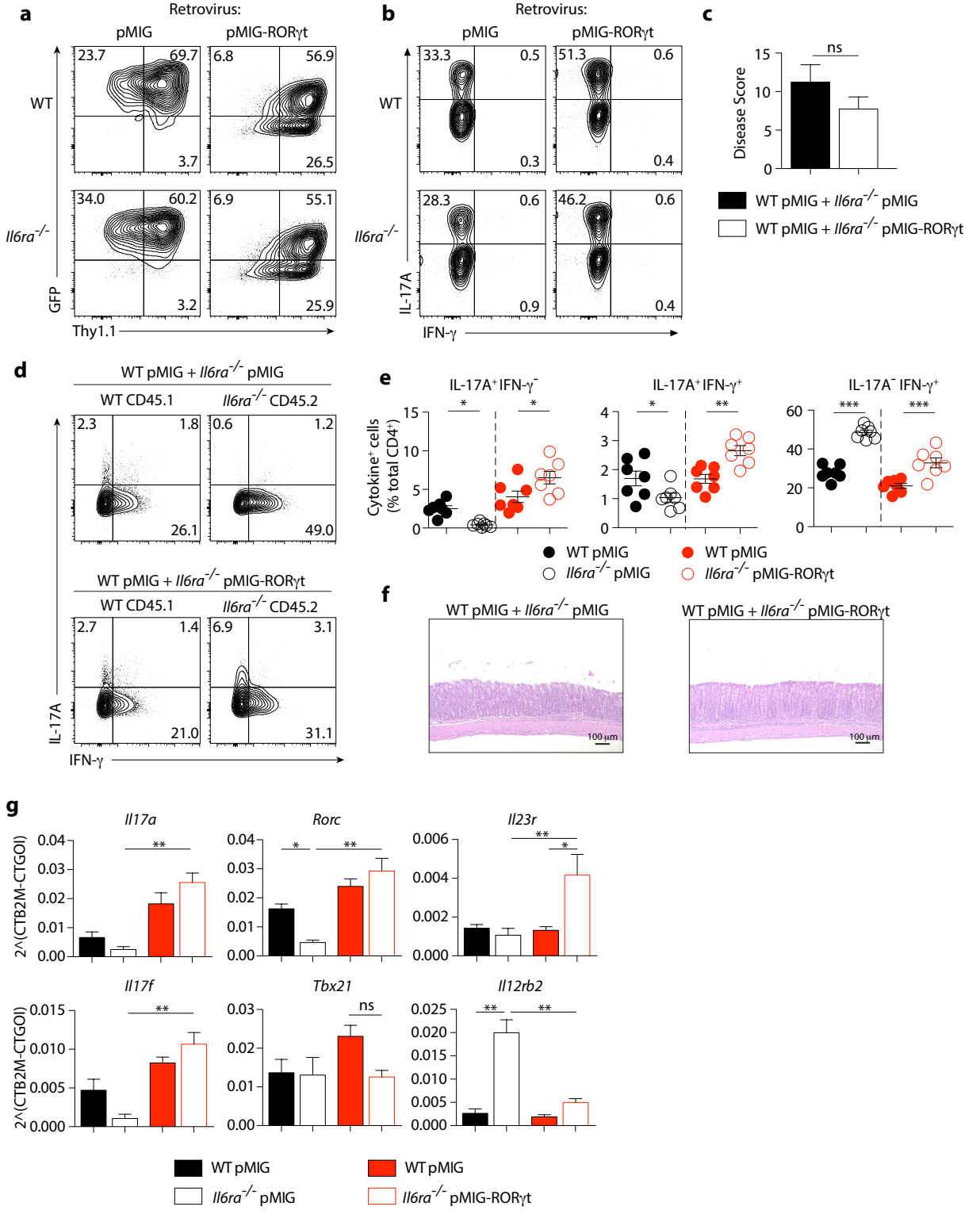

Fig. 7. Enforced RORγt expression represses transition to Th1-like cells by IL-6Rα-deficient Th17 precursors in vivo. (**A**) CD4+ T cells from *Il17f*$^{thy1.1}$ CD45.1 (WT) and *Il6ra*$^{-/-}$ *Il17f*$^{thy1.1}$ (*Il6ra*$^{-/-}$)

were cultured under Th17 polarizing conditions (2.5 ng/ml TGF-β, 10 μg/ml anti-IFN-γ, 10 μg/ml anti-IL-4, 10 ng/ml HDS) with CD3/CD28 expander beads (ThermoFisher) and transduced with retroviruses encoding GFP alone (pMIG) or GFP with RORγt (pMIG- RORγt). FACS plots show GFP and Thy1.1 expression on D6 and are gated on $CD4^+$ T cells. (**B**) Th17p were stained intracellularly for IL-17A and IFN-γ after PMA/Ionomycin activation for 5 h in the presence of monensin. FACS plots are gated on $CD4^+$ GFP^+ $Thy1.1^+$ cells. (**C**) GFP^+ $Thy1.1^+$ Th17 cells from (**A**) were FACS purified and transferred together (2 x 10^5 each/mouse) into *Rag1*$^{-/-}$ recipients (WT pMIG + *Il6ra*$^{-/-}$ pMIG n = 7, WT pMIG + *Il6ra*$^{-/-}$ pMIG-RORγt n = 7). Histological scores were analyzed three weeks after transfer (mean + SEM). (**D**) Representative FACS plots showing IL-17A and IFN-γ in CLP $CD4^+$ T cells from recipients of co-transfers *ex vivo* after development of colitis. (**E**) Relative frequencies of IL-$17A^+$, IL-$17A^+$ IFN-γ^+, and IFN-γ^+CD4^+ T cells in the CLP of colitic mice (mean ± SEM). * $P < 0.05$, ** $P < 0.01$, *** $P < 0.001$. (**F**) Representative H&E stained sections of colon from recipients of WT pMIG + *Il6ra*$^{-/-}$ pMIG or WT pMIG + *Il6ra*$^{-/-}$ pMIG-RORγt $CD4^+$ T cells. H&E stain; original magnification 10x; scale bars 100 μm. (**G**) RNA isolated from FACS purified WT and *Il6ra*$^{-/-}$ CLP $CD4^+$ T cells from co-transfer recipients was analyzed *ex vivo* by qPCR for expression of *Il17a*, *Il17f*, *Rorc*, *Tbx21*, *Il12rb2* and *Il23r* (mean + SEM of three biological replicates). * $P < 0.05$, ** $P < 0.01$. Data are representative of three experiments. P values; one-way ANOVA with Tukey's multiple comparison test (**G**) or one-way ANOVA with Bonferroni post test (**E**) .

Supplementary Materials:

Supplementary Fig. 1. Classical IL-6 signaling is required for development of colitis.

Supplementary Fig. 2. Innate derived IL-6 is required for Th17 pathogenicity and maintenance.

Supplementary Fig. 3. Classical IL-6 signaling is required for maintenance of Th17 cells.

Supplementary Fig. 4. Co-transfer of *Il6ra*$^{-/-}$ with WT Th17 cells is unable to rescue their phenotype.

Supplementary Fig. 5. Co-transfer of *Il6ra*$^{-/-}$ with WT Th17 cells is unable to rescue their Th17 phenotype.

Supplementary Fig. 6. IL-6Ra and gp130 expression on Th17 cells ex vivo.

Supplementary Fig. 7. *Il6ra*$^{-/-}$ Th17 cells lose their Th17 gene expression signature in vivo.

Supplementary Table 1. Full gene sets used for GSEA analysis.

Supplemental Figures

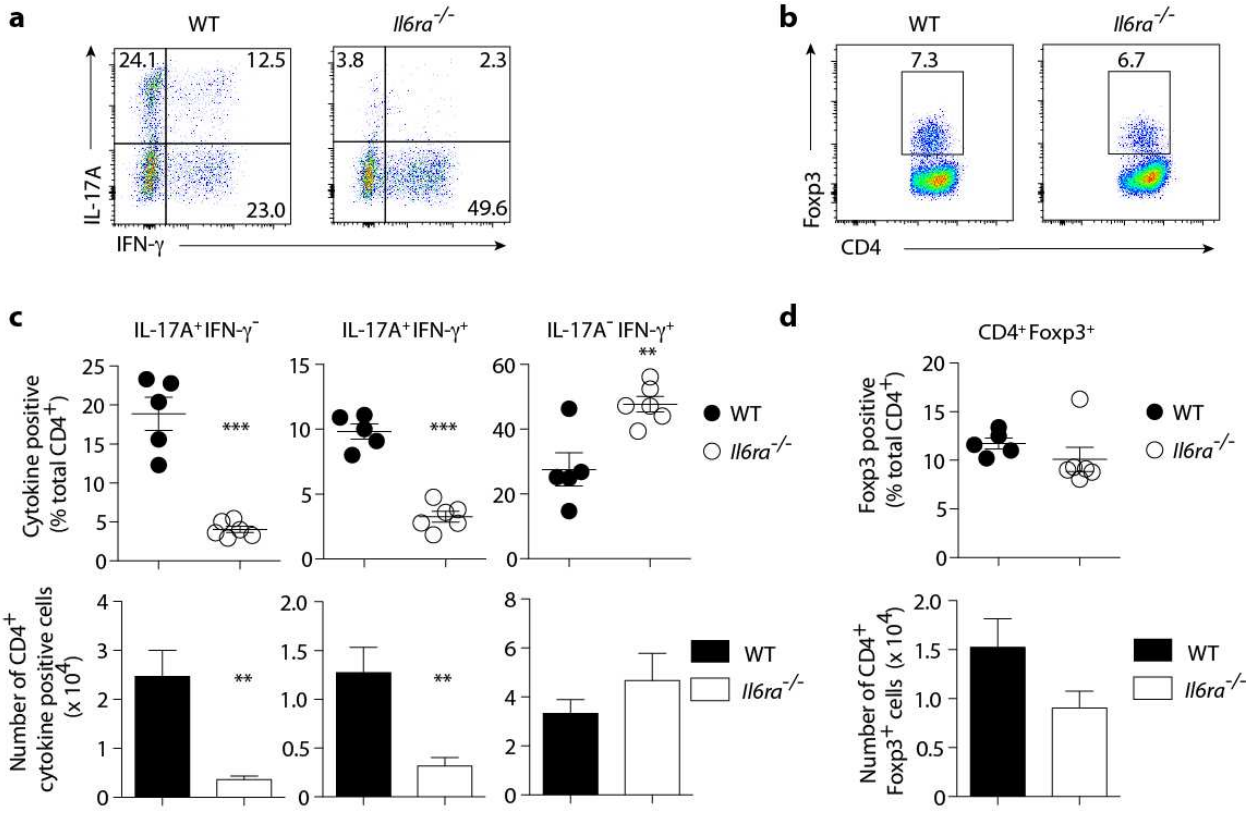

Supplementary Fig. 1. Classical IL-6 signaling is required for development of colitis. FACS sorted $CD4^+$ $CD45RB^{Hi}$ T cells isolated from WT and *Il6ra*$^{-/-}$ mice were transferred into *Rag1*$^{-/-}$ recipients (4×10^5 per mouse)(WT n = 5 per group, *Il6ra*$^{-/-}$ n = 6 per group) and analyzed for colitis 8 weeks after transfer. (**A**) Representative FACS plots showing IL-17A and IFN-γ in MLN $CD4^+$ T cells ex vivo after development of colitis. (**B**) Representative FACS plots showing Foxp3 expression in MLN $CD4^+$ T cells ex vivo from WT or *Il6ra*$^{-/-}$ recipients after development of colitis. (**C**) Relative frequencies (upper) and total numbers (lower) of IL-$17A^+$, IL-$17A^+$IFN-γ^+, and IFN-γ^+ $CD4^+$ T cells in the MLN of colitic mice (mean ± SEM). *** P <0.0001, *** P <0.0001, ** P = 0.0045 (upper IL-$17A^+$, IL-$17A^+$IFN-γ^+, and IFN-γ^+CD4^+ T cells). ** P = 0.002, ** P = 0.0046, P = 0.3380 (lower IL-$17A^+$, IL-$17A^+$IFN-γ^+, and IFN-γ^+CD4^+ T cells) (**D**) Relative frequencies (upper) and total numbers (lower) of $Foxp3^+$ $CD4^+$ T cells from the MLN (mean ± SEM). P = 0.2940 (upper), P = 0.0887 (lower). P values; unpaired two-tailed Student's t-test (**C** - **D**).

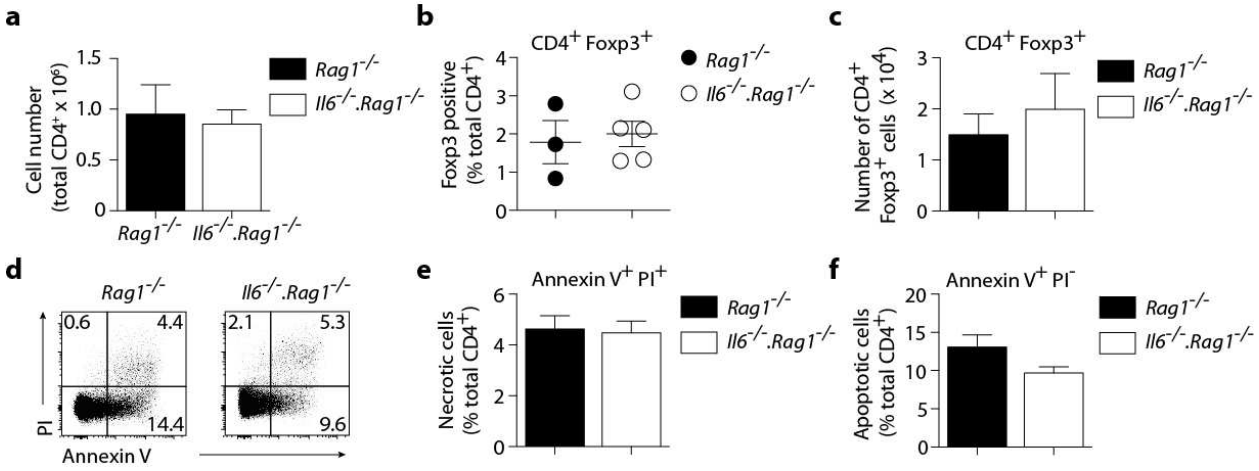

Supplementary Fig. 2. Innate derived IL-6 is required for Th17 pathogenicity and maintenance. (**A**) Total numbers of CD4+ T cells recovered from the CLP of *Rag1*-/- (n = 4) or *Il6*-/-.*Rag1*-/- (n = 8) recipients (mean + SEM). (**B**-**C**) Relative frequencies (**B**) and total numbers (**C**) of Foxp3+ CD4+ T cells from the CLP of *Rag1*-/- or *Il6*-/-.*Rag1*-/- recipients (mean ± SEM). (**D**) Representative FACS plots showing expression of Annexin V and Propidium Iodide (PI) in CD4+ T cells recovered from the CLP of colitic *Rag1*-/- or *Il6*-/-.*Rag1*-/- recipients. (**E-F**) Relative percentages of necrotic (Annexin V+ PI+) (**E**) and apoptotic (Annexin V+PI-) (**F**) CD4+ T cells from the CLP of colitic *Rag1*-/- or *Il6*-/-.*Rag1*-/- recipients (mean + SEM).

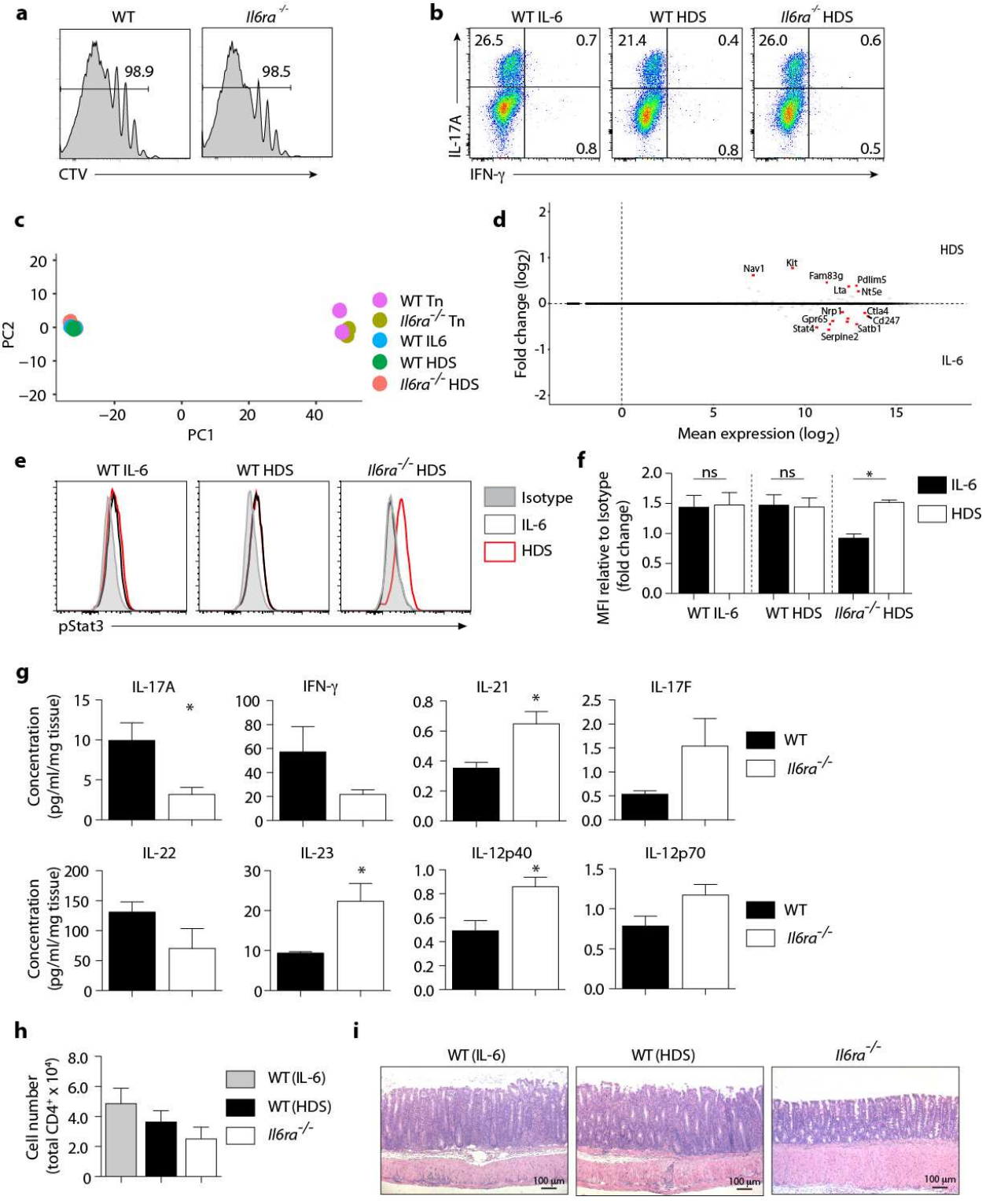

Supplementary Fig. 3. Classical IL-6 signaling is required for maintenance of Th17 cells. (**A**) CD4+ T cells from *Il17f*$^{thy1.1}$ (WT) and *Il6ra*$^{-/-}$. *Il17f*$^{thy1.1}$ (*Il6ra*$^{-/-}$) were labeled with Cell Trace Violet

(CTV; ThermoFisher) and cultured with irradiated splenic feeder cells under Th17 polarizing conditions for 7 d with 10 ng/ml recombinant hIL-6. A fraction of cells were analyzed for expression of CD4 and CTV dilution. FACS plots are gated on $CD4^+$ $Thy1.1^+$ Th17 cells. (**B**). $CD4^+$ T cells from *Il17f*$^{Thy1.1}$ (WT) and *Il6ra*$^{-/-}$. *Il17f*$^{Thy1.1}$ (*Il6ra*$^{-/-}$) were cultured with irradiated splenic feeder cells under Th17 polarizing conditions with 10 ng/ml IL-6 or 10 ng/ml recombinant IL-6-sIL6Ra (HDS) for 7 d. A fraction of cells was analyzed for expression of CD4 and intracellular IL-17A and IFN-γ after PMA/Ionomycin stimulation for 5 hr in the presence of monensin. FACS plots are gated on $CD4^+$ cells. (**C**) 6 days after culture, Thy1.1+ Th17 precursors were isolated and gene expression analyzed by RNA seq. Plot shows PCA analysis of mRNA transcriptome in naïve and in vitro Th17 polarized WT (IL-6), WT (HDS) and Il6ra-/- (HDS) CD4+ T cells by RNA-seq analysis. Each dot represents an individual mouse. Data are from two independent experiments. (**D**) MA plot displays differentially expressed genes in WT (HDS)(upper) and WT (IL-6)(lower) $CD4^+$ T cells *ex vivo*. Red circles indicate genes with false discovery rate (FDR) <0.05. (**E**) $CD4^+$ T cells from *Il17f*$^{Thy1.1}$ (WT) and *Il6ra*$^{-/-}$. *Il17f*$^{Thy1.1}$ (*Il6ra*$^{-/-}$) were cultured with irradiated splenic feeder cells under Th17 polarizing conditions with 10 ng/ml IL-6 or 10 ng/ml recombinant IL-6-sIL6Ra (HDS). On day 5, Th17 cells were stimulated with equimolar concentrations of IL-6 or HDS (0.95nM) for 15 min. Representative FACS plots show pSTAT3 (Y705) in in vitro polarized Th17 cells. (**F**) Fold change of pSTAT3 (Y705) MFI (GeoMean) relative to isotype control (mean + SEM) from three independent experiments. * $P < 0.05$, one-way ANOVA with Bonferroni post-test. (**G**) Colon culture explant supernatants from *Rag1*$^{-/-}$ recipients of WT or *Il6ra*$^{-/-}$ Th17 cells (n = 3 per group) were assayed for select cytokines by Luminex assay (Millipore) four weeks after transfer. Data are expressed as pg/mg/ml tissue (mean + SEM) and represent one of two independent experiments. IL-17A * $P = 0.048$, IFN-γ $P = 0.1742$, IL-21 * $P = 0.0303$, IL-17F $P = 0.1573$, IL-22 $P = 0.1366$, IL-23 * $P = 0.0465$, IL-12p40 * $P = 0.0328$, IL-12p70 $P = 0.0997$. *P* values; unpaired two-tailed Student's *t*-test.

(**H**) Total number of CD4+ T cells isolated from the CLP of Rag1-/- recipients of WT (IL-6), WT (HDS) or Il6ra-/- Th17p cells four weeks after transfer (mean + SEM). (**I**) Representative H&E

stained sections of colon from *Rag1*$^{-/-}$ recipients of WT (IL-6)(left), WT (HDS)(middle), or Il6ra-/- Th17p (right) WT Th17 cells. H&E stain; original magnification 10x; scale bars 100 μm.

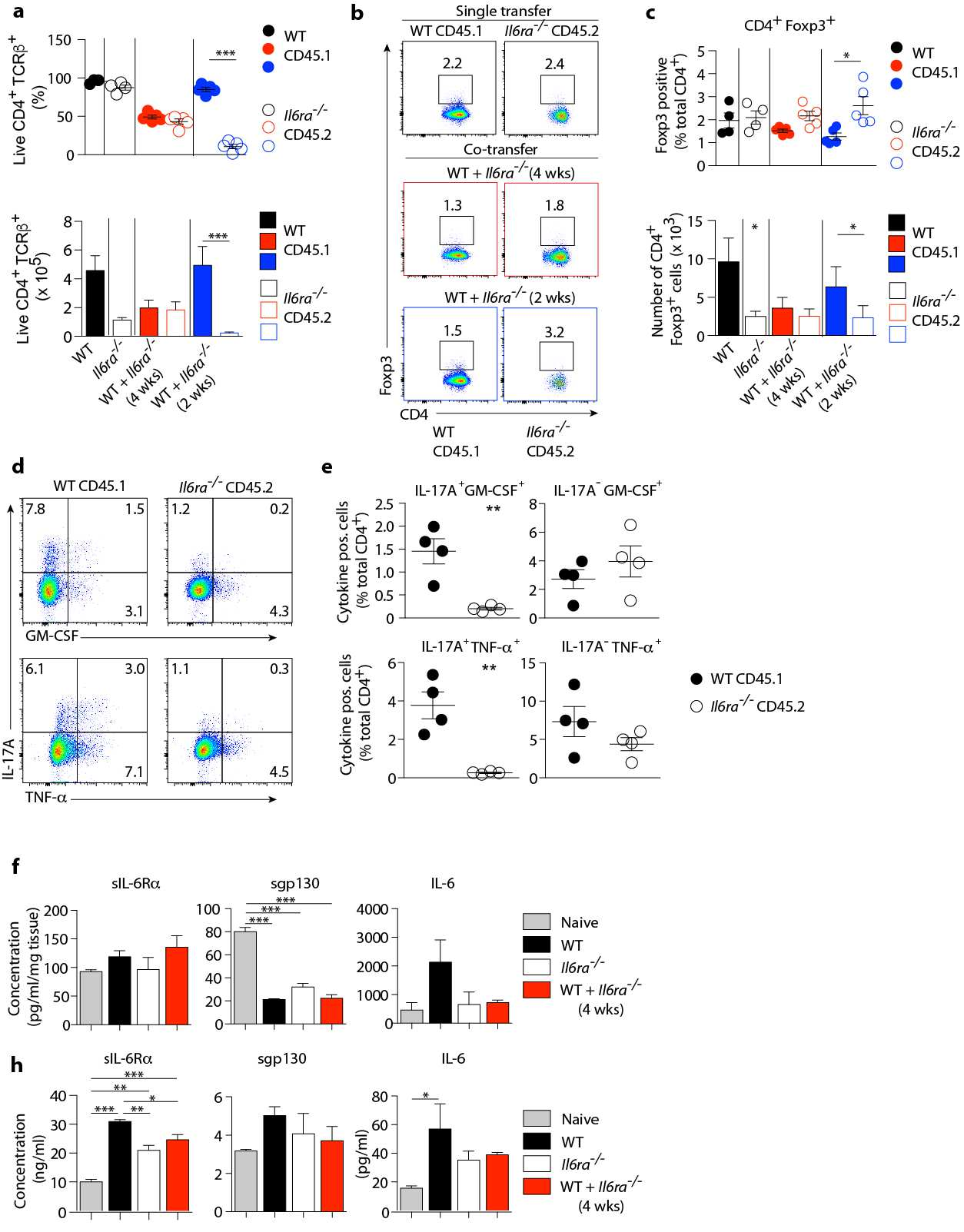
a
Live CD4+ TCRβ+ (%)
WT
CD45.1
Il6ra-/-
CD45.2
***
Live CD4+ TCRβ+ (x 10^5)
WT
Il6ra-/-
WT + Il6ra-/- (4 wks)
WT + Il6ra-/- (2 wks)
b
Single transfer
WT CD45.1
Il6ra-/- CD45.2
2.2
2.4
Co-transfer
WT + Il6ra-/- (4 wks)
1.3
1.8
WT + Il6ra-/- (2 wks)
1.5
3.2
Foxp3
CD4
c
CD4+ Foxp3+
Foxp3 positive (% total CD4+)
Number of CD4+ Foxp3+ cells (x 10^3)
d
WT CD45.1
Il6ra-/- CD45.2
7.8
1.5
3.1
1.2
0.2
4.3
6.1
3.0
7.1
1.1
0.3
4.5
GM-CSF
IL-17A
TNF-α
e
IL-17A+GM-CSF+
IL-17A- GM-CSF+
IL-17A+TNF-α+
IL-17A- TNF-α+
Cytokine pos. cells (% total CD4+)
**
WT CD45.1
Il6ra-/- CD45.2
f
sIL-6Rα
sgp130
IL-6
Concentration (pg/ml/mg tissue)
Naive
WT
Il6ra-/-
WT + Il6ra-/- (4 wks)
h
sIL-6Rα
sgp130
IL-6
Concentration (ng/ml)
(pg/ml)
Naive
WT
Il6ra-/-
WT + Il6ra-/- (4 wks)

Supplementary Fig. 4. Co-transfer of *Il6ra*$^{-/-}$ with WT Th17 cells is unable to rescue their phenotype. (**A**) Relative percentage (upper) and total numbers (lower) of CD4^{+} T cells recovered from the CLP of colitic recipients of WT, *Il6ra*$^{-/-}$ or WT + *Il6ra*$^{-/-}$ co-transfers of Th17 cells (mean + SEM). (**B**) Representative FACS plots showing expression of Foxp3 in recovered CD4+ T cells from the CLP of colitic mice. (**C**) Relative frequencies (upper) and total number (lower) of CD4+ Foxp3+ cells in the CLP of colitic recipients of WT, *Il6ra*$^{-/-}$ or WT + Il6ra$^{-/-}$ Th17 co-transfers (mean ± SEM). (**D**) Representative FACS plots showing expression of IL-17A, TNF-α and GM-CSR in recovered CD4^{+} T cells from the CLP of colitic mice. (**E**) Relative percentage of IL-17A^{+}GM-CSF^{-}, GM-CSF^{+} (upper), IL-17A^{+}TNF-α^{+}, and TNF-α^{+} CD4^{+} T cells in the CLP of colitic mice (mean ± SEM). ** $P < 0.01$ (unpaired two-tailed Student's *t*-test). (**F**-**G**) Levels of sIL-6Ra, sgp130 and IL-6 in colon explants (**F**) and serum (**G**) of naive *Rag1*$^{-/-}$ mice as well as colitic recipients of single or co-transfer Th17 cells were quantified by Milliplex assay (mean + SEM). Data are representative of two independent experiments (WT n = 4, *Il6ra*$^{-/-}$ n = 4, WT + *Il6ra*$^{-/-}$ n = 5, WT + *Il6ra*$^{-/-}$ (2 wks) n = 5). * $P < 0.05$, ** $P < 0.01$, *** $P < 0.001$ (one-way ANOVA with Bonferroni post-test).

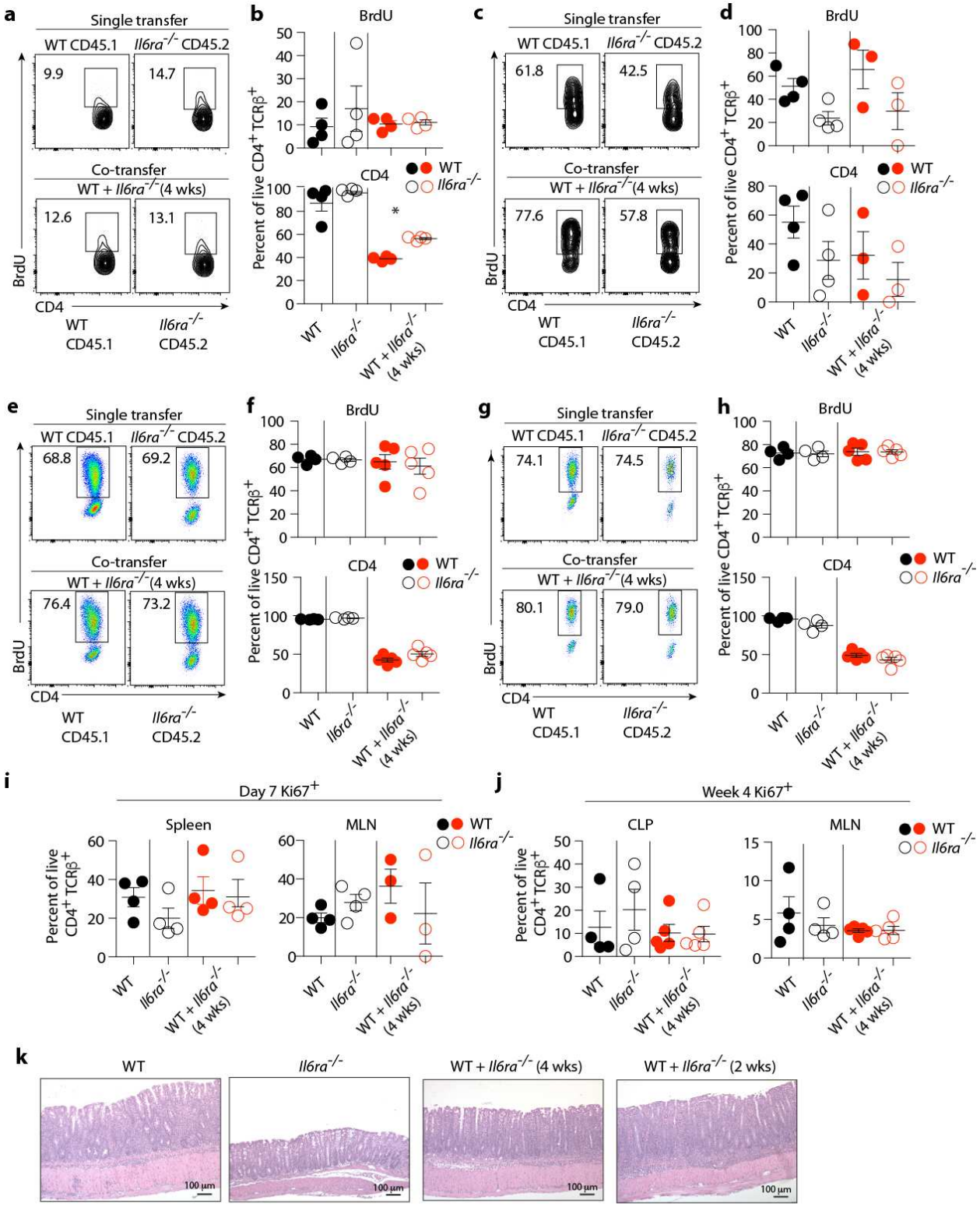
a
Single transfer
WT CD45.1
Il6ra-/- CD45.2
9.9
14.7
Co-transfer
WT + Il6ra-/- (4 wks)
12.6
13.1
BrdU
CD4
WT CD45.1
Il6ra-/- CD45.2
b
BrdU
Percent of live CD4+ TCRβ+
CD4
WT
Il6ra-/-
*
WT
Il6ra-/-
WT + Il6ra-/- (4 wks)
c
Single transfer
WT CD45.1
Il6ra-/- CD45.2
61.8
42.5
Co-transfer
WT + Il6ra-/- (4 wks)
77.6
57.8
BrdU
CD4
WT CD45.1
Il6ra-/- CD45.2
d
BrdU
Percent of live CD4+ TCRβ+
CD4
WT
Il6ra-/-
WT
Il6ra-/-
WT + Il6ra-/- (4 wks)
e
Single transfer
WT CD45.1
Il6ra-/- CD45.2
68.8
69.2
Co-transfer
WT + Il6ra-/- (4 wks)
76.4
73.2
BrdU
CD4
WT CD45.1
Il6ra-/- CD45.2
f
BrdU
Percent of live CD4+ TCRβ+
CD4
WT
Il6ra-/-
WT
Il6ra-/-
WT + Il6ra-/- (4 wks)
g
Single transfer
WT CD45.1
Il6ra-/- CD45.2
74.1
74.5
Co-transfer
WT + Il6ra-/- (4 wks)
80.1
79.0
BrdU
CD4
WT CD45.1
Il6ra-/- CD45.2
h
BrdU
Percent of live CD4+ TCRβ+
CD4
WT
Il6ra-/-
WT
Il6ra-/-
WT + Il6ra-/- (4 wks)
i
Day 7 Ki67+
Spleen
MLN
Percent of live CD4+ TCRβ+
WT
Il6ra-/-
WT
Il6ra-/-
WT + Il6ra-/- (4 wks)
j
Week 4 Ki67+
CLP
MLN
Percent of live CD4+ TCRβ+
WT
Il6ra-/-
WT
Il6ra-/-
WT + Il6ra-/- (4 wks)
k
WT
Il6ra-/-
WT + Il6ra-/- (4 wks)
WT + Il6ra-/- (2 wks)
100 μm

Figure S5

Supplementary Fig. 5. Co-transfer of *Il6ra*$^{-/-}$ with WT Th17 cells is unable to rescue their Th17 phenotype. *Rag1*$^{-/-}$ mice (n = 4 per group) were adoptively transferred with 4 x 10^5 WT or *Il6ra*$^{-/-}$ Th17 cells or co-transferred with 2 x 10^5 WT + *Il6ra*$^{-/-}$ Th17 cells. Recipient mice were fed with water containing 1 mg/ml Bromodeoxyuridine (BrdU) for 7 days. (**A** and **C**). Representative FACS plots show BrdU staining of CD4+ T cells recovered from the spleens (**A**) and MLN (**C**) of single and co-transfer Th17 cell recipients 7 days after transfer. (**B** and **D**) Relative percentage of BrdU$^+$ CD4$^+$ cells (upper) and total CD4$^+$ cells (lower) in the spleen (**B**) and MLN (**D**) of single and co-transfer Th17 recipients 7 days after transfer (mean ± SEM). (**E** and **G**) Representative FACS plots showing BrdU staining of CD4$^+$ T cells recovered from the CLP (**E**) and MLN (**G**) of single and co-transfer Th17 cell recipients 4 weeks after transfer. (**F** and **H**) Relative percentage of BrdU$^+$ CD4$^+$ cells (upper) and total CD4+ cells (lower) in the CLP (**F**) and MLN (**H**) of single and co-transfer Th17 recipients 4 weeks after transfer (mean ± SEM). (**I**) Relative percentages of CD4$^+$ Ki67$^+$ cells in the spleen (left) and MLN (right) of recipient mice 7 days after transfer (mean ± SEM). (**J**) Relative percentages of CD4$^+$ Ki67$^+$ cells in the CLP (left) and MLN (right) of recipient mice 4 weeks after transfer (mean ± SEM). (**K**) Representative H&E stained sections of colon from recipients of (left to right) WT, *Il6ra*$^{-/-}$, WT + *Il6ra*$^{-/-}$ (4 wks) and WT + *Il6ra*$^{-/-}$ (2 wks) CD4+ T cells. H&E stain; original magnification 10x; scale bars 100 μm. Data are representative of two independent experiments. * $P < 0.05$ (one-way ANOVA with Bonferroni post-test).

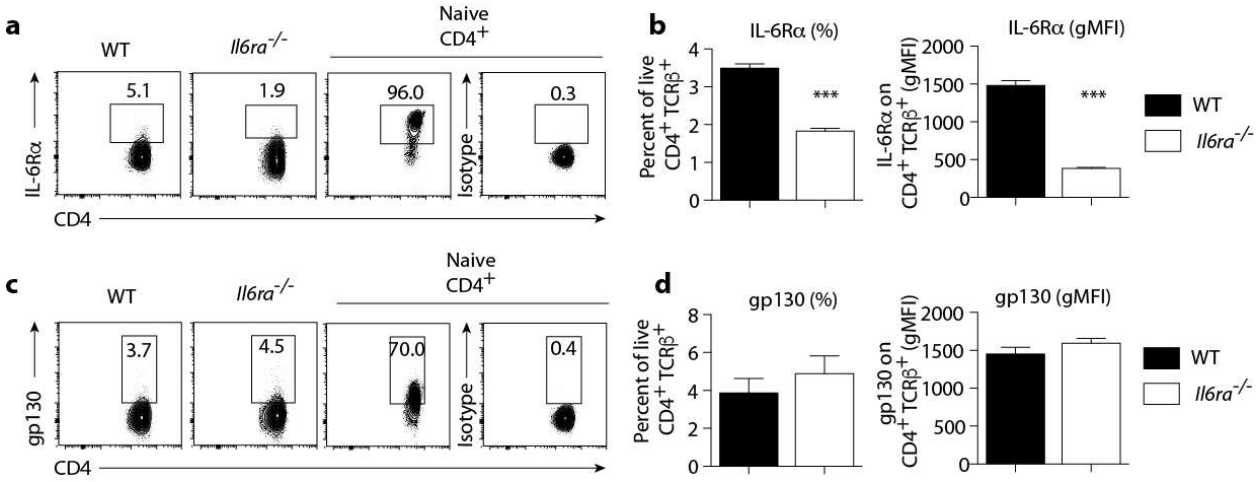

Supplementary Fig. 6. IL-6Ra and gp130 expression on Th17 cells ex vivo. (**A**) Representative FACS plots showing IL-6Ra expression in CLP CD4+ T cells ex vivo, 4 weeks after *Rag1*-/- recipients were co-transferred with WT and *Il6ra*-/- Th17 cells (n = 4 per group). (**B**) Relative percentage (left) and geometric mean fluorescence (right) of CD4+ IL-6Ra+ cells in CLP CD4+ T cells ex vivo. *** P <0.0001. (**C**). Representative FACS plots showing gp130 expression in CLP CD4+ T cells ex vivo. (**D**). Relative percentage (left) and geometric mean fluorescence (right) of CD4+ gp130+ cells in CLP CD4+ T cells ex vivo (mean + SEM). Data are representative of two independent experiments. P values; unpaired two-tailed Student's t-test.

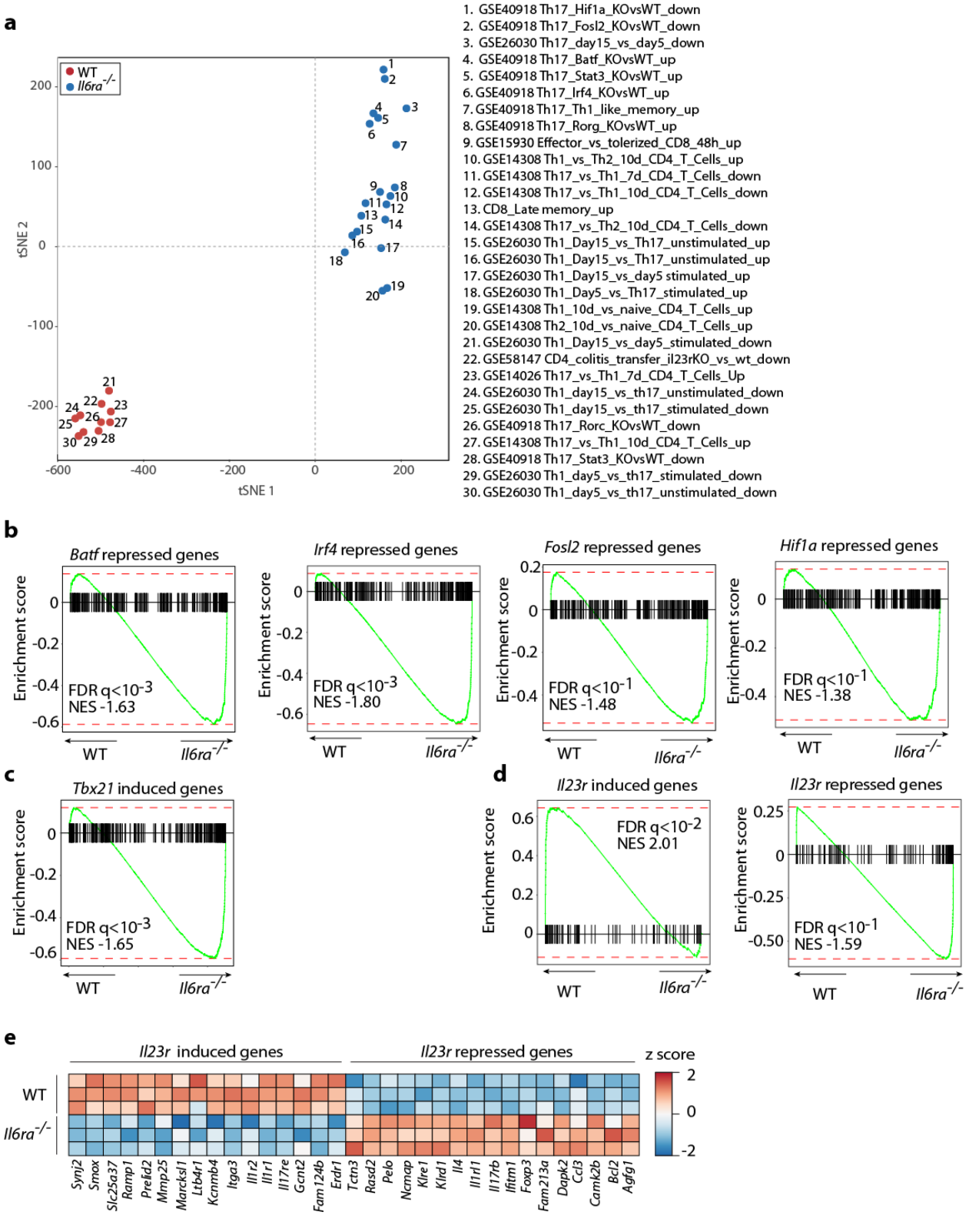
a
WT
Il6ra-/-
tSNE 2
tSNE 1
1. GSE40918 Th17_Hif1a_KOvsWT_down
2. GSE40918 Th17_Fosl2_KOvsWT_down
3. GSE26030 Th17_day15_vs_day5_down
4. GSE40918 Th17_Batf_KOvsWT_up
5. GSE40918 Th17_Stat3_KOvsWT_up
6. GSE40918 Th17_Irf4_KOvsWT_up
7. GSE40918 Th17_Th1_like_memory_up
8. GSE40918 Th17_Rorg_KOvsWT_up
9. GSE15930 Effector_vs_tolerized_CD8_48h_up
10. GSE14308 Th1_vs_Th2_10d_CD4_T_Cells_up
11. GSE14308 Th17_vs_Th1_7d_CD4_T_Cells_down
12. GSE14308 Th17_vs_Th1_10d_CD4_T_Cells_down
13. CD8_Late memory_up
14. GSE14308 Th17_vs_Th2_10d_CD4_T_Cells_down
15. GSE26030 Th1_Day15_vs_Th17_unstimulated_up
16. GSE26030 Th1_Day15_vs_Th17_unstimulated_up
17. GSE26030 Th1_Day15_vs_day5 stimulated_up
18. GSE26030 Th1_Day5_vs_Th17_stimulated_up
19. GSE14308 Th1_10d_vs_naive_CD4_T_Cells_up
20. GSE14308 Th2_10d_vs_naive_CD4_T_Cells_up
21. GSE26030 Th1_Day15_vs_day5_stimulated_down
22. GSE58147 CD4_colitis_transfer_il23rKO_vs_wt_down
23. GSE14026 Th17_vs_Th1_7d_CD4_T_Cells_Up
24. GSE26030 Th1_day15_vs_th17_unstimulated_down
25. GSE26030 Th1_day15_vs_th17_stimulated_down
26. GSE40918 Th17_Rorc_KOvsWT_down
27. GSE14308 Th17_vs_Th1_10d_CD4_T_Cells_up
28. GSE40918 Th17_Stat3_KOvsWT_down
29. GSE26030 Th1_day5_vs_th17_stimulated_down
30. GSE26030 Th1_day5_vs_th17_unstimulated_down
b
Batf repressed genes
Irf4 repressed genes
Fosl2 repressed genes
Hif1a repressed genes
Enrichment score
FDR q<10-3
NES -1.63
FDR q<10-3
NES -1.80
FDR q<10-1
NES -1.48
FDR q<10-1
NES -1.38
WT
Il6ra-/-
c
Tbx21 induced genes
FDR q<10-3
NES -1.65
d
Il23r induced genes
Il23r repressed genes
FDR q<10-2
NES 2.01
FDR q<10-1
NES -1.59
e
Il23r induced genes
Il23r repressed genes
z score
Synj2
Smox
Slc25a37
Ramp1
Prelid2
Mmp25
Marcksl1
Ltb4r1
Kcnmb4
Itga3
Il1r2
Il1r1
Il17re
Gcnt2
Fam124b
Erdr1
Tctn3
Rasd2
Pelo
Ncmap
Klre1
Klrd1
Il4
Il1rl1
Il17rb
Ifitm1
Foxp3
Fam213a
Dapk2
Ccl3
Camk2b
Bcl2
Agfg1

Supplementary Fig. 7. *Il6ra*$^{-/-}$ Th17 cells lose their Th17 gene expression signature in vivo. (**A**) Similarity of gene sets calculated by the Jaccard index. Dimensions were reduced to two with t-SNE and visualized with a scatterplot. (**B**) Barcode plots of gene set enrichment results obtained using sets of genes previously reported to be regulated by several Th17 transcription factors (GSE 40918). (**C**) Barcode plots of gene set enrichment results obtained using a set of genes regulated by *Il23r* in Th17 cell (GSE 58147). (**D**) Expression of representative genes identified by gene set enrichment in (**C**) are depicted by heat map with z-scored values. Data are from two independent experiments.